Chapter 1: Introduction

The spatial and temporal distributions of shallow landslides are important components of the natural and management-related disturbances in mountain drainage basins (Selby, 1993; Guzzetti *et al.*, 1999). The sudden failure and high speed of shallow landslides makes them potentially destructive to downstream resources, property and human lives (Selby, 1993). In an attempt to minimise negative impact of landslides, various research efforts have been directed towards early warning systems for evacuating neighbourhoods (Liao and Xu., 1997; Iiritano *et al.*, 1998). Infrastructure, such as roads, buildings (Alexander, 1989) and bridges have construction requirements to make them as safe as possible if affected by landslides.

In an international realm landslides are responsible for thousands of annual casualties (Selby, 1993). In comparison, no loss of life has been documented in South Africa (Paige-Green, 1989). Alexander (1992) describes a landslide that supposedly killed six Lesotho men. According to Alexander (1992) the storm during which the landslide took place is still remembered amongst the Lesotho people as 'Lijabatho' – The Devourer of Men'. Annual economical damage resulting from landslides in South Africa in the late 1980's was estimated to be in the region of US$ 20 million (United States Dollars) for landslide prevention and rehabilitation (Paige-Green, 1989). Although Paige-Green's (1989) work is more than 13 years old, it is the only synthesis available for comparison with other countries such as the USA where damage resulting from landslides during 2000 was estimated to be US$ 5869 million while the annual average figure for India is US$ 1000 million (Glade, 1998).

In South Africa, landslides tend to occur in mountainous regions experiencing a high rainfall frequency. Paige-Green (1989) constructed a landslide susceptibility map based on the rainfall, water surplus, geomorphic provinces, geology and engineering reports in South Africa (Figure 1.1). Areas that are highly susceptible to landslides are the Western Cape mountains, the eastern coastal regions and the mountainous areas of Lesotho and the KwaZulu-Natal Drakensberg. High landslide susceptibility within mountainous nature reserves (Western Cape and KwaZulu-Natal) have no direct threat to people and this explains why there are not many recorded incidences of landslides, as noted by Paige-Green (1989).

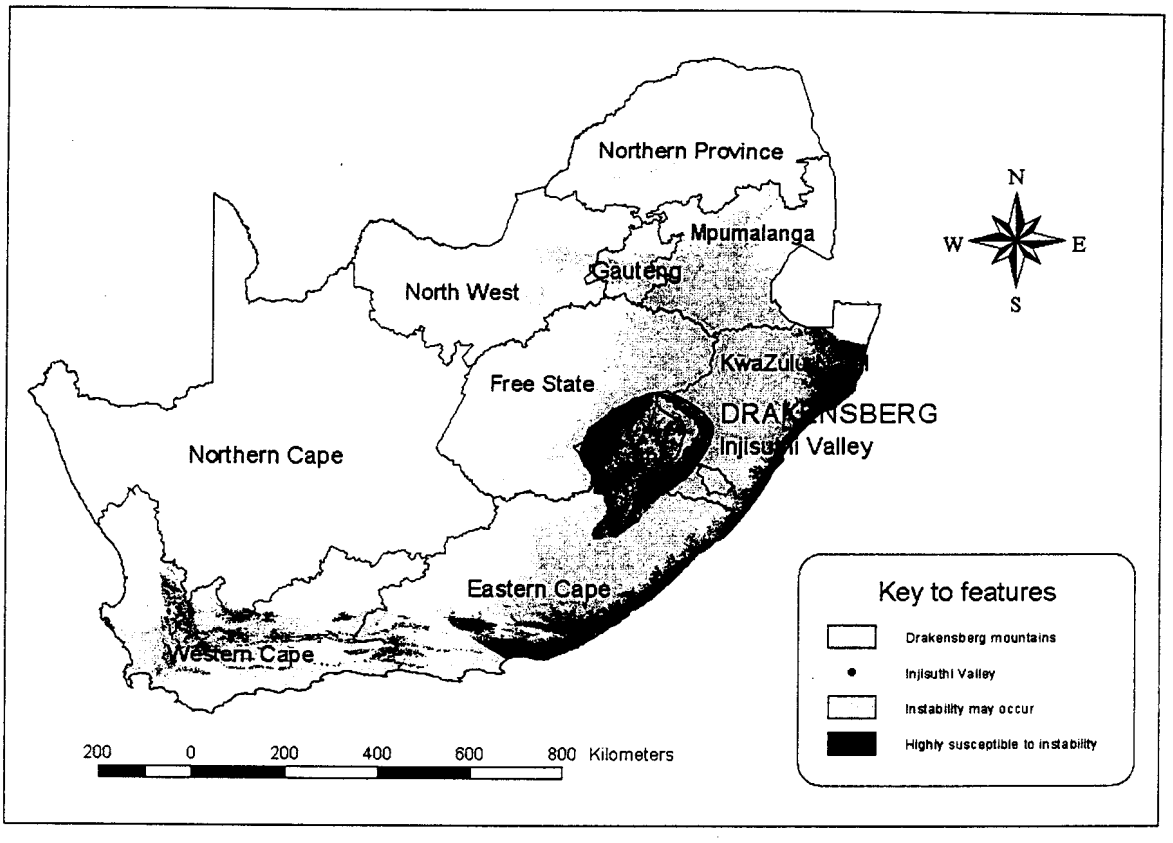

Figure 1.1: Landslide susceptibility zones in South Africa based on rainfall, water surplus, geomorphic provinces, geology and engineering reports (after Paige-Green, 1989).

In South Africa, relatively little is known on the nature and distribution of landslides (Beckedahl *et al.*, 1988); small-scale studies have focussed on the engineering instability of slopes where information is usually contained in confidential engineering reports (*e.g.* Hands, 1973; Brink, 1983; Webb and Mival, 1983; Pegram and Adamson, 1988). Landslides as a geomorphologic phenomenon in South Africa have been studied by Beckedahl *et al.* (1988); Garland and Olivier (1993); Olivier *et al.* (1993) and Sumner (1993); studies on landslides are descriptive in nature and to date no known research has been done on the dynamic modelling of landslides in South Africa.

1.1 Retrospect of modelling in physical geography

Given the absence of published landslide models within South Africa there is a need for research based on contemporary developments in physical modelling. Models in physical geography have been developed since the early 1960's and the development of the theory, conceptual thoughts and technology are described by Thornes (1989) and summarised below.

1.1.1. Theoretical developments

The production of *Models, Paradigms and the New Geography* by Haggett and Chorley (1967) signalled the beginning of the end of a decade of effort to shift geomorphology from a largely qualitative subject towards a quantitative and process oriented discipline (Thornes, 1989). According to Thornes (1989), the past preoccupation in geomorphology focussed on reconstruction based on speculative connections between landforms and sediments on the one hand and past climate on the other. The shift in discipline was towards the investigation of field processes, statistical analysis of general morphometric data and the acceptance of mathematical modelling (Thornes, 1989). Some important precursors of the paradigm shift include Strahler's advocacy of systems analysis (1950) and the dynamic basis of geomorphology (1952), Culling's (1957) introduction of the relevance of systems theory and its relationship to fluvial and hill slope processes as well as Scheidegger's (1961) contribution to the analytical modelling of hillslope processes and form.

Theoretical developments in landslide modelling have been characterised by a number of important contributions. For example, slope stability processes that are modelled in combination with hydrological contributions are recognised in three key papers by Kirkby (1967, 1971, 1980). The first concerned the theoretical development of the influence of topography on the nature and location of through flow (Kirkby and Chorley, 1967). This led to investigations on the contribution of topographically controlled slope water movement (Anderson and Burt, 1978), the understanding of subsurface water movement in relation to solute chemistry (Burt *et al.*, 1983), and the development of general hydrological model of ungauged catchments (Beven and Kirkby, 1978). The second paper (Kirkby, 1971) concerned the development of characteristic profiles for hillslopes given a continuity-base process model. The third paper (Kirkby, 1980) further developed Smith and Bretherton's (1972) concept of the stability of hillslope hollows to produce a verifiable model of the controls of climate, lithology, topography and basal slope dynamics on drainage density as a function of drainage network growth. The key papers in hillslope stability briefly discussed above form the basis for most contemporary landslide modelling.

1.1.2. Conceptual developments

In addition to the theoretical developments of modelling, there have been a number of important conceptual advances that have strengthened the modelling approach to geomorphology. Thornes (1989) highlights the difference between systems and models where systems actually exist (though can never be completely described). A model is said to be an attempt to describe, analyse, simplify or display systems. The systems approach was codified for physical geographers by Chorley and Kennedy (1971) and thoroughly reviewed by Bennett and Chorley (1978). In addition to the theory of dynamic systems, the concept of thresholds and instability were also developed for modelling, initially conceived and formalised in a geomorphic context by Smith and Bretherton (1972) and later illustrated and popularised by Schumm (1973).

In recent years modelling and the concept of geomorphometry (or simply morphometry) has become popular as the study of numerical representation of topography, and involves sciences such as mathematics, geomorphology, geography and computing (Pike, 1995). Geomorphometry greatly assisted the development of physical models in geography and is widely applied to hillslope forms and landslide prediction models (Pike, 1995).

1.1.3. Technical developments

A third type of change that is responsible for the development of modelling in geomorphology is technical. Thornes (1989) describes the situation during the 1960's when differential equations and analytical methods were not as available as they are today. However, the availability of relatively cheap, fast, user-friendly computing power as well as software for numerical computations was revolutionary. Development of numerical techniques for handling spatially complex distributed models has displaced all the strategies of the seventies for modelling geomorphic systems (*e.g.* Ahnert, 1976; Armstrong, 1976). An important consequence of lifting the restrictions imposed by computer hardware and software is the development of very large-scale systems simulations such as the U.S.'s water erosion model developed by the National Soil Erosion Laboratory (1995). The availability of comprehensive spatial data sets on the Internet and CD-ROM for digital elevation models, soils, land use and climate has stimulated the development of procedures for processing the data into useful forms for modelling, in terms of atmospheric, soil, ground and surface water (Maidment, 1996). According to Maidment (1996) the emphasis in hydrological modelling in a GIS is on

the digital description of the environment, and then on the formulation of process models that can fit the available data and environmental description. Maidment (1996) argues for a reversal of the traditional priorities of hydrological modelling, where the emphasis is on the hydrology and not on the environmental characteristics.

Technological developments that have contributed towards landslide modelling include the use of remote sensing imagery for identifying landslides and record detail for their monitoring (*e.g.* McDermid and Franklin, 1995). Brunsden (1993), however, notes that the poor resolutions of satellite imagery make landslides smaller than 60m by 60m difficult to detect. Other technology such as the Global Positioning System (GPS) has also been used to monitor slow moving large-scale (approximately 1km long) landslides in China with success (*e.g.* Kodama *et al.*, 1997), but is inappropriate for small scale landslide predictions.

Development in software and particularly the introduction of computerised Digital Elevation Models (DEMs) by Miller and Laflamme (1958), are being increasingly used by geomorphologists and hydrologists (*e.g.* Da Ros and Borga, 1997) for mathematical analysis of landscapes and or the modelling of surface processes (Desmet, 1997). A DEM offers the most common method for extracting vital topographic information and even enables the routing of flow across topography (Kirkby, 1990). Topography is a controlling factor in distributed models of landform processes such as slope stability (*e.g.* Niemann and Howes, 1991; Moore *et al.*, 1988; Dietrich *et al*, 1993, Van Asch *et al.*, 1993; Desmet, 1997) and must be represented as accurately as possible. Accuracy and data quality management in GIS has also received increasing attention as shown in the bibliography of Burger and López (1994). The accuracy of DEM and software defines the limit to accuracy for landslide model prediction.

Research on the accuracy of DEM in the modelling of mass movements has focused on issues such as error in DEM's with regard to the density and distribution of the sample points (Li, 1992), methods used for the acquisition of data (Fryer *et al.*, 1994) and terrain characteristics (Li, 1992). Interpolation of DEM's in a GIS has also received attention, where research on their accuracy includes the work of Guth (1995), who derived DEM's using six different algorithms. Nogami (1995) introduces an algorithm for deriving DEM from topographic maps and López (1997) classified types of random errors in DEM's. Accuracy comparisons between triangular irregular network (TIN) and

digital elevation model (DEM) have also received attention within the ongoing vector versus raster debate in GIS.

Two main approaches that use digital terrain data (DEM) to represent the spatial distribution of slope instability are outlined by Montgomery and Dietrich (1994). One involves generating topographic attributes for digital terrain data (*e.g.* slope) that can be combined with other characteristics such as vegetation or lithology in a GIS to identify hazardous areas based on the observed correlation between landsliding and their attributes (Carrarra *et al.*, 1991). This method classifies relatively large areas into stability types, rather than resolve fine-scale patterns of instability that would be particularly valuable for hazard assessment in land management. Moreover, such models tend to be site specific because of the empirical basis of GIS based multivariate analysis. The other approach is to use digital elevation data to make process-based predictions of site instability. Okumura and Nakagawa (1988) used a grid-based DEM in a finite difference model of shallow subsurface flow under steady rainfall. Predicted pressure values were used to calculate the stability of individual grid cells using a form of the infinite slope model. Although many more cells were predicted to be unstable than were actually observed, their model correctly identified most of the scars in a small (0.1km^2) study catchment. The second method is widely applied in contemporary landslide modelling (e.g. Montgomery and Dietrich, 1994; Borga *et al.*, 1998).

1.2 Model categories

Models in physical geography have in the past been classified in various categories, for example, Kirkby (1989) describes 3 main types as the 'black-box', 'physically based' and 'stochastic' models. According to Kirkby (1989) black box models are widely used for forecasting; for example the universal soil loss equation (USLE). The physical and stochastic models are discussed as part of the classification of Huggett (1985) that also defines three major model types: (1) conceptual, (2) scale and (3) mathematical models (Figure 1.2). A conceptual model is a mental image (*e.g.* a map or block diagram) or an equation of a natural phenomenon (*e.g.* infinite slope model) in which the essential features of the phenomenon are retained and details regarded as extraneous are excluded. Scale models are physically based models in which both materials and the stresses acting on them should be scaled in proportion. Mathematical models represent the features of a system by abstract symbols and their

interactions are replaced by expressions containing mathematical variables, parameters and constants (Selby, 1993). Mathematical models can also be subdivided into three classes (Figure 1.2). Stochastic and statistical models both have a random process incorporated. However, in statistical models the unpredictable data is from naturally variable phenomena such as rainfall and soils, while the stochastic model describes a system based on assigned probability. Deterministic models are conceptual models in mathematical form, but without the random component, that may be derived from physical or chemical principles or from experimental and observational data. Different model types are not mutually exclusive.

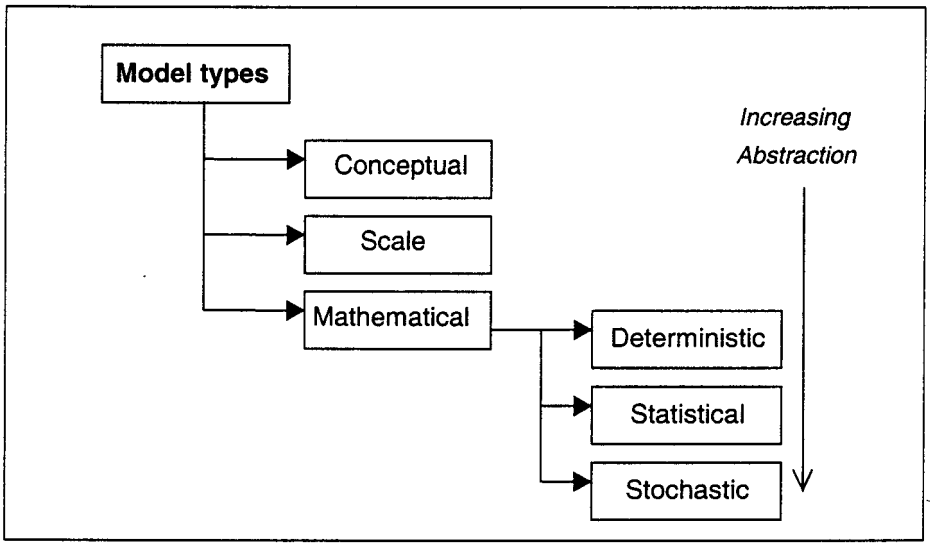

Figure 1.2: Some model types based partly on the classification of Huggett (1985), Selby (1993) and Thomas and Huggett (1980).

According to Van Westen and Terlien (1996), one of the prerequisites for a deterministic slope stability model is that the geomorpological and geological conditions should be fairly homogeneous over the entire study area and that the landslide types should be simple (or translational) as opposed to complex rotational landslides. Advantages of a sound physically based model are that it is readily transferable between sites, on the basis of site measurements that should be explicitly related to the model parameters (Kirkby, 1989). The main objection to the use of physically-based models is that they require a large amount of data for model calibration and verification (Terlien, 1996). Laboratory measurements of the strength values of the soils that serve as model inputs are also time consuming (Van Asch *et al.*, 1993). Terlien (1996) argues that the study of Kirkby (1988) which distributed

physically–based models shows little forecasting advantage over simpler approaches. Therefore, there has been a renewed interest in simpler models in which processes of minor importance are treated in a more conceptually ordered way. Van Asch *et al.* (1993), however, argue that traditional qualitative maps or statistical maps require the same density of data in order to achieve the same accuracy obtained by two-dimensional physically based models and that physically based models produce better results than simpler techniques.

In deterministic models, it is possible to analyse the sensitivity of the equilibrium system for different landslide parameters. The effective changes of parameters in different scenarios (*e.g.* amount of rainfall) for the degree of stability can be simulated (Van Asch *et al.*, 1993). According to Van Asch *et al.* (1993) the use of a large scale DEM in deterministic models for landslide stability will result in accurate landslide hazard zonation.

Stochastic models used in landslide hazard prediction include probabilities of elevation uncertainty in GIS (Ehschlaeger and Shortridge, 1996) and uncertainty in defining categorical maps and data management errors (Ehschlaeger and Goodchild, 1994). Error propagation modelling, however, falls outside the scope of this project. According to Van Asch *et al* (1993) the most accurate and realistic model calculations are based on probability analysis of slope stability (in other words a stochastic model). Statistical and deterministic analysis of landslide factors based on the presence or absence of landslides is also a successful method of landslide modelling although this does not automatically result in the assessment of the degree of hazard, the maps produced by statistical models are reliable with respect to predicting potential unstable areas (Van Asch *et al.*, 1993).

1.3 Dimensions of modelling

Model types have different dimensions based on their time-space scales and mathematical calculations. Deterministic models, compiled in a Geographic Information System (GIS) may have one-, two-, or three-dimensions. The most complex calculation procedure, using three dimensional slope stability programs, requires the sampling of data at predefined grid-points and the exportation of data to an external three-dimensional slope stability model (Van Westen and Terlien, 1996). A one-dimensional deterministic model, based on the infinite slope model has wide

applications (*e.g.* Ward *et al.*, 1982) is said to be the most suitable method for landslide prediction (Van Westen and Terlien, 1996). However, with the expanding capabilities of GIS, the quantification of topographic attributes of a landscape through the combined use of the digital elevation model (DEM) and infinite slope model made two-dimensional slope stability programs possible. DEM's depict the convergence and divergence of flow lines, which result in spatial variations of soil moisture. Two-dimensional models can further identify source areas of subsurface flow (Terlien, 1996), saturation excess overland flow (Burt and Butcher, 1985), topographic hollows, convergence of flow, preferential sites for runoff generation (O'Loughlin, 1986), all of which are significant considerations in landslide hazard zonation.

1.4 Landslide hazard zonation

Landslide hazard zonation is the classification of a terrain into safe and unsafe areas according to the probability and/or the incidence of landslides and other mass-movements (Varnes, 1984). Maps depicting landslide hazard zonation are generally used for land-use planning and the development of appropriate remedial measures where there is a potential for economic damage or loss of life (*e.g.* Sarkar *et al.*, 1995). Use of the word "hazard" refers to a threat to humans and is not applicable to the modelling of naturally occurring landslides that do not pose a direct economic or safety to people. Shallow landslides occurring in the KwaZulu-Natal Drakensberg conservation areas (Figure 1.1) seldom pose a significant hazard to people or property and therefore the term landslide susceptibility zonation rather than a landslide hazard zonation is more appropriate for this process. Principles for the preparation of susceptibility maps are similar to those of the hazard map initiated by the United States Geological Survey (*e.g.* the work done by Brabb *et al.*, 1972, cited in Sarkar *et al.*, 1995) and extended by Kienholz (1978) and Ives and Bovis (1978).

Various approaches to landslide hazard zonation modelling have been used in the past, and can be grouped into five main categories as summarised by Guzzetti *et al.* (1999). The first two methods are direct and qualitative, while the last three are indirect and quantitative.

(1) Geomorphological hazard mapping as a qualitative method relies on the ability of the investigator to estimate actual and potential slope failures (Mejía-Navarro, 1993).

(2) The heuristic approach to landslide hazard zonation modelling is based on the prior knowledge of all causes and instability factors of landsliding in the area under investigation. It is an indirect, mostly qualitative method, that depends on how well and how much the investigator understands the geomorphological processes acting in the area (Guzzetti *et al.*, 1999). Instability factors are ranked and weighted according to their assumed or expected importance in causing mass movement (Guzzetti *et al.*, 1999).

(3) Analysis of landslide scars and deposit inventories to delineate potentially hazardous areas. Predictions of future instability patterns are based on the occurrence of past and present landslide deposits (Van Steijn and Van Den Hof, 1983).

(4) Statistical approach involving examples of multivariate analysis (Cararra, 1983; Guzzetti, 1993), principle component analysis (Neuland, 1976), or correlation coefficients of factors characterising observed sites of slope instability (Garland and Olivier, 1993).

(5) Stability rating based on geometric, geological and structural attributes (Shroder, 1998). These models are process-based and rely upon the understanding of physical laws controlling slope instability (Montgomery and Dietrich, 1994; Borga *et al.*, 1998; Gritzner *et al.*, 2001). In recent years, delineation of potential landslide hazard has been greatly facilitated with the use of GIS. A GIS efficiently organises spatially distributed data in digital format, allowing rapid assessment of spatial correlation between different data types and extraction of pertinent topographic information. The combination of statistical techniques and GIS is frequently used for example logistic regression in landslide hazard analysis (Gorsevski *et al.*, 2000). Physically based and geotechnical models retain the essence of the physical controls of topography, soil properties and triggering factors, such as rainfall, but that remain parametrically simple for the ease of calibration (Van Asch *et al.*, 1993). The latter modelling approach is feasible for the evaluation of shallow landslide occurrence because certain aspects of the surface topography, which are readily extracted form high-resolution digital elevation (DEM) data, act as primary controls on the initiation of shallow landslides. According to Borga *et al.* (1998) such models use site-specific information, and may resolve patterns of instability at a finer scale than is possible with empirical hazard mapping.

1.5 Slope stability factors

The distinction between stable and unstable areas on a landslide hazard zonation map is influenced by various slope stability factors. According to Selby (1993) soil water quantity changes and the associated pore pressure changes are the main factors responsible for the triggering, the re-triggering and the velocity of landslides. Rainfall triggered landslides are, *per* definition, shallow and translational (Sidle *et al.*, 1985). Landslides are primarily influenced by five factors, namely, pore water pressure, soil density, soil cohesion, angle of internal friction and slope angle (Mulder, 1991). Various secondary factors that may influence the slope stability include the soil structure and geology (Mejía-Navarro, 1993; Onda, 1993), chemical processes, glacial influences and seismic activity (Keefer *et al.*, 1979; Larsen, 1995) as well as the inclination of undisturbed slopes (i.e. gravity). Every slope experiences the influence of gravity, and together with the changes of other slope characteristics, natural and anthropogenic agents can cause changes in the mass of the slope material. Changes in the primary and secondary factors affecting slope stability have a temporal and spatial significance for the landslide processes.

1.6 Research problem

Models have heuristic value in the study of the natural mechanisms involved in landsliding. Although some descriptive studies have been done, there are no known models that predict the natural occurrence of landslides in South Africa. In the Injisuthi Valley shallow landsliding pose economic losses in the form of localised road failure, that could be prevented if zones of potential slope instability were outlined beforehand in the form of a landslide susceptibility map. A landslide susceptibility map can be obtained through the dynamic modelling of hydrological and physical factors involved in shallow landsliding. The importance of modelling, as a contemporary research direction as discussed will yield a better understanding of the spatial and temporal processes involved in slope instability.

1.6.1 Aim and objectives

The aim for this study is to produce a landslide susceptibility map derived from the hydrological and physically based modelling of factors that interact to cause the natural occurrence of landslides in the Injisuthi Valley, KwaZulu-Natal Drakensberg. The model will attempt spatial prediction of landslides based on specific physical environmental properties and the hydrology of the area. A Geographic Information System (GIS) will serve as the framework in which the spatial data will be collected and analysed. If the model is successful, it can be used as a planning tool for management of the KwaZulu-Natal Parks.

The aim will be achieved through meeting the following objectives:

- The measurement of important environmental variables related to landsliding identified by Mulder (1991).
- Classification of landslides.
- Development of a computer model script in PCRaster Dynamic Modelling Package (Utrecht University, 1994). The model will have both a soil mechanical and a hydrological focus.
- Sensitivity analysis and calibration of model inputs to optimise model predictions.
- Model confirmation by comparing the actual position of landslides to the predicted position in the study area.
- Model validation by assessing predictive power at an independent validation area.
- Production of landslide susceptibility map.

1.7 Project outline

Following the overview of landslides and modelling provided above, Chapter 2 presents the general environmental, climatic and geological setting of the Injisuthi Valley, central KwaZulu-Natal Drakensberg, and highlights the nature, extent and geomorphic significance of contemporary mass movements processes. Chapter 3 describes the environmental parameters that are used for model inputs, their measurement and the fieldwork findings as well as their conversion to landslide prediction model input maps or constants. A landslide morphometric inventory is also used to classify the dominant landsliding process as a basis for selecting relevant mathematical equations for constructing a landslide model script. Chapter 4 outlines the mathematical background and assumptions of the landslide susceptibility model. Digital topographic maps and the computer derivation of the slope angle and local

drainage direction are included and programming language script of the landslide prediction model is presented. Chapter 5 describes the statistical procedures for model sensitivity analysis and constant calibration. Model confirmation is achieved by comparing landslide predictions against observed landslide locations in the study area. The model is also independently verified at a separate north-facing site in the Injisuthi Valley. Various statistical methods are used express of the accuracy of the model predictions. The model is also compared to two existing GIS hydrological slope stability models and the differences in constructions and accuracy of predictions are compared. In Chapter 6 comments on the validity of the model for the prediction of landslides in the Injisuthi Valley are made and prospective model usage and improvements highlighted.

Chapter 2: Study site

The Drakensberg Mountains in the province of KwaZulu-Natal form a continuous crescent-shaped escarpment situated between 160km and 240km inland of the eastern coast of South Africa (Figure 1.1). The escarpment creates a natural watershed that is the boundary between eastern Lesotho and South Africa (between latitudes 28.50°S and 30.50°S and longitudes 28.50°E and 29.50°E) (Figure 2.1). The site selected for investigation into landslides was in the Injisuthi Valley, situated in the northern corner of the Giant's Castle Game Reserve (between latitude 29.09° to 29.14° S and longitude 29.41° to 29.50° E). "Injisuthi", a Zulu word meaning 'well fed dogs' is a conservation area managed by KwaZulu-Natal Wildlife as a tourist destination with a range of recreation opportunities and spectacular mountain scenery.

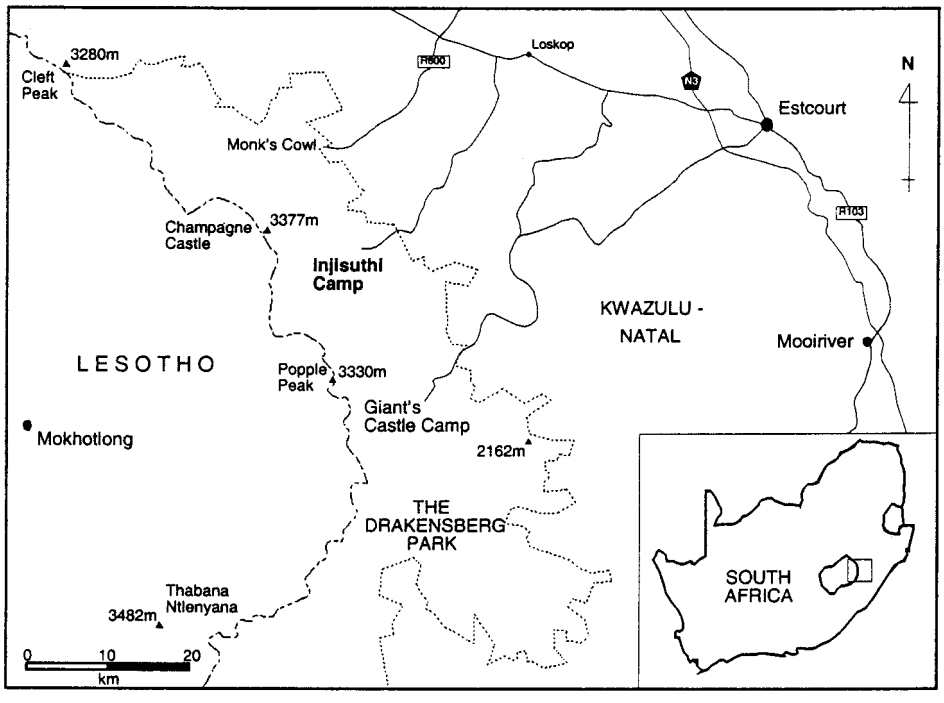

Figure 2.1: Location of the Injisuthi Valley in KwaZulu-Natal.

2.1 Geology

The geology of the Drakensberg comprises two clearly defined areas consistent throughout the mountain range, east of the escarpment. First, the summit area and gigantic basalt scarp of volcanic origin rising from about 2000 meters to in excess of 3000 meters comprises the Main Escarpment (Figure 2.2). This is superimposed on a

sandstones stretching from the floor of river valleys at approximately 2000m to 1250m, capped with several layers of sandstone known as the Little Berg (Figure 2.2).

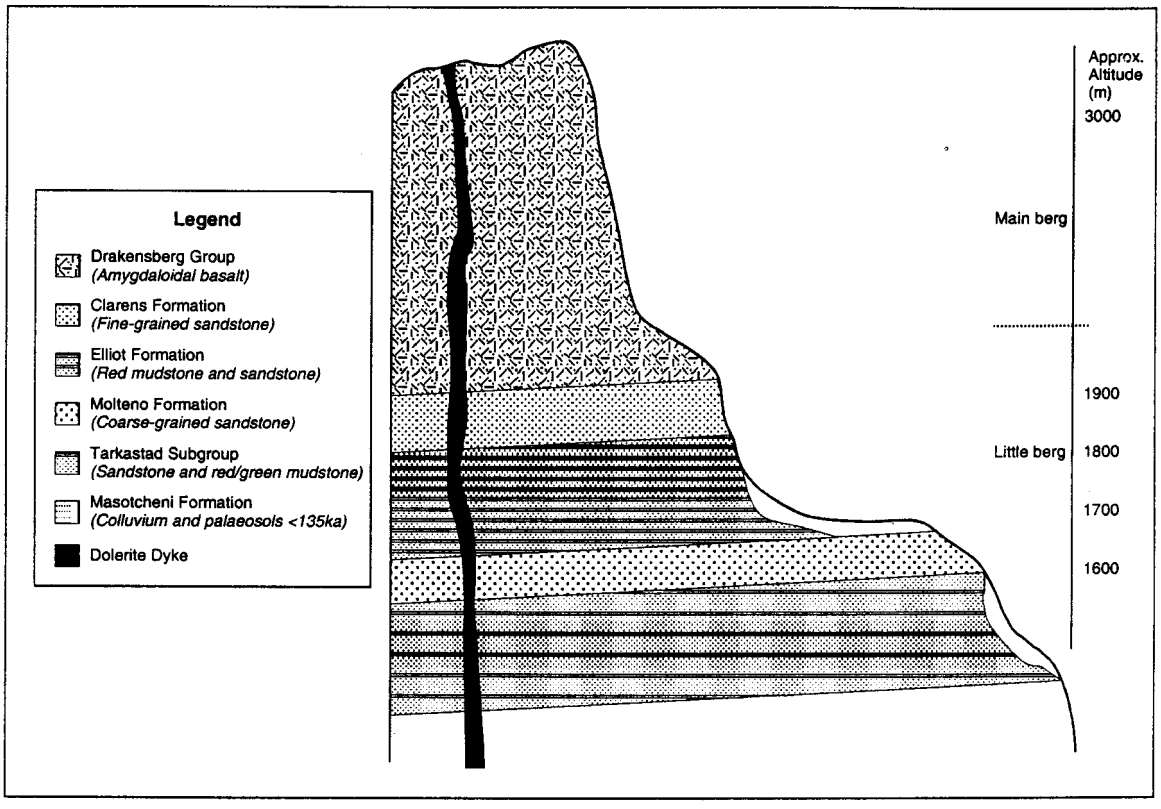

Figure 2.2: Profile through the Drakensberg showing the Little and Main Berg geological formations (after Pickles, 1985).

The Little Berg primarily comprises of three sandstone formations, namely Clarens, Elliot and Molteno overlaying outcrops of the Beaufort series in the valley floors. Differences in the sandstone formations are distinguished by the varying degrees of mud and clay content (Table 2.1) and are important in determining susceptibility to mass movement processes in the area. For example, a higher mud content in the soils (e.g. those overlaying the Elliot and Molteno formations) will increase water retention and load the slopes more than sandy soils, and making the slopes more susceptible to failure, as is often noted in the Injisuthi Valley.

Table 2.1: Stratigraphical sequence in the Injisuthi Valley (after Ericksson, 1983).

Super-group	Group	Formation	Lithology	Thickness (m)	Elevation range (m a.s.l.)
Karoo super-group	Drakensberg (volcanics)	-	Basalt	900	2000 - 3000
	No group name	Clarens	Sandstone	55	1710 - 2000
		Elliot	Red mudstone with lenses of sandstone	210	1580 – 1710
		Molteno	Sandstone and grey mudstone	45	1480 – 1580
	Beaufort	-	Sandstone	100	1380 - 1480

Thicknesses of all the sedimentary formations, Molteno, Elliot and Clarens formations, vary greatly throughout the Drakensberg and the two first named thin out rapidly form south to north (Table 2.1). The strata of the formations in the KZN Drakensberg (Figure 2.2) all rest in a near horizontal position with a dip that is seldom steeper than 6° south to south-westerly direction (Stockley, 1947). Small structural domes and basins in the strata are considered to be the result of intrusions of sills into the underlying formations (Nixon, 1973) (Figure 2.2).

2.2 Soils

To date no comprehensive study of the soils of the KZN Drakensberg has been undertaken. Soil classification of the Tugela basin by Van Der Eyk *et al.* (1969) focuses on the basaltic strata of the Main berg and excludes the 'rather inaccessible' and agriculturally less relevant Little Berg and Escarpment zones. Some small-scale soil studies at Cathedral Peak Research Station (Schulze, 1974; Granger, 1976) describe the soils of the Little Berg as ferrallitic, structureless and acid due to a high degree of leaching. The soils surveyed by Schulze (1974) and Granger (1976) have developed on basaltic strata and follow the soil classification terminology by Van Der Eyk *et al.* (1969) who identifies five dominant soils namely Mispah, Clovelly, Hutton, Griffin and Katspruit. In Mispah soils the A horizons rest directly on the bedrock and have a mean depth of 11 cm (where they do not consist of rocky outcrops). The other soil forms are distinguished in the B horizon which can be yellow apedal (Clovelly), red apedal (Hutton), yellow and red apedal (Griffin) or firm gley (Katspruit) (Van Der Eyk *et al.*, 1969). According to Van Der Eyk *et al.* (1969), Hutton and Griffin soils occur on

slops with lower gradients, whilst Katspruit soils are acid hydromorphic and described to occur on poorly drained valley floors and in narrow strips along streams.

2.3 Geomorphology

Interpretations of the geomorphic evolution of the Main Berg (Figure 2.1) are summarised by Boelhouwers (1988a) and range from faulting, scarp retreat, erosion surfaces to Pliocene uplift. During the Pliocene uplift, described by King (1982), fluvial incision resulting in the rejuvenation of streams caused slope over steepening resulting in deep-seated mass-movement events (Sumner and Meiklejohn, 2000). Recently, the contribution of periglacial processes in the high Drakensberg (Boelhouwers, 1991, 1994) and the cryogenic influence that may have extended down the Main Escarpment in the last glacial, in the form of a niche glacier, give some evidence for cryogenic processes at lower altitudes (De Villiers, 2000; Boelhouwers and Meiklejohn (in press)). Some research on the evolution of the main suggested that parallel escarpment retreat is the result of mass movement (Munro-Perry, 1990) and erosion (Boelhouwers, 1988a). According to Sumner (1997) the contribution of landslides to the geomorphology of the Drakensberg is apparently little understood.

2.3.1 Dolerite dykes and deep-seated landslides

One of the major causes of deep-seated paleo-landslides that involve bedrock and major rotational slumping in the Injisuthi Valley are the position of dolerite sills and dykes. Dolterite dykes are intrusions of Karoo dolerite occur extensively throughout the Injisuthi Valley and have a dominant north-west and south-east preferential direction while the intensity of sheet intrusions are in the north-west direction where there are more weaknesses in the earth crust (Figure 2.2) (Linström, 1981; Meiklejohn, 2000). Linear dykes have lengths varying more than 30km and thickness ranging between 1 to 15m (Linström, 1981). Major landslides in the Injisuthi Valley have been noted to be of complex origin involving material that generally comprises of debris of sandstone clasts and slump blocks in a loamy matrix. Boelhouwers (1992) measured the widths of typical major landslides in Giant's Castle Game Reserve to range from 140m to 300m, with maximum thickness of the deposits between 25m to 50m. Many major rotational landslides associated with dolerite dykes in the Injisuthi Valley are relict and the whole valley is a paleo-landslide zone upon which contemporary surficial landslides occur. Some larger rock falls have been noted to occur biennually (Wight[1]).

2.3.2 Surficial landslides

Minor surficial translational (Figure 2.3) and rotational landslides are apparently not influenced by the position of the dolerite dykes in the Injisuthi Valley. Instead, they are triggered by the liquefying effect of water and include hillslope materials such as rock fragments and soils that move gravitationally downward and outward (Radbruch-Hall and Varnes, 1976). Instability and recurring landslides have economic implications for the management of the area, indicated by the road failures on unstable slopes (Figure 2.4). Changes in the slope angle as a result of hillslope excavation, changes in drainage as well as loading of the slope with tar may be triggering factors for landslides. A landslide prediction model could be potentially useful in identifying the zones of instability prior to road construction and other developments. Previous mass movements in the valley have been at a far greater scale and the most frequent mass wasting activity that is observed is in the form of shallow landslides.

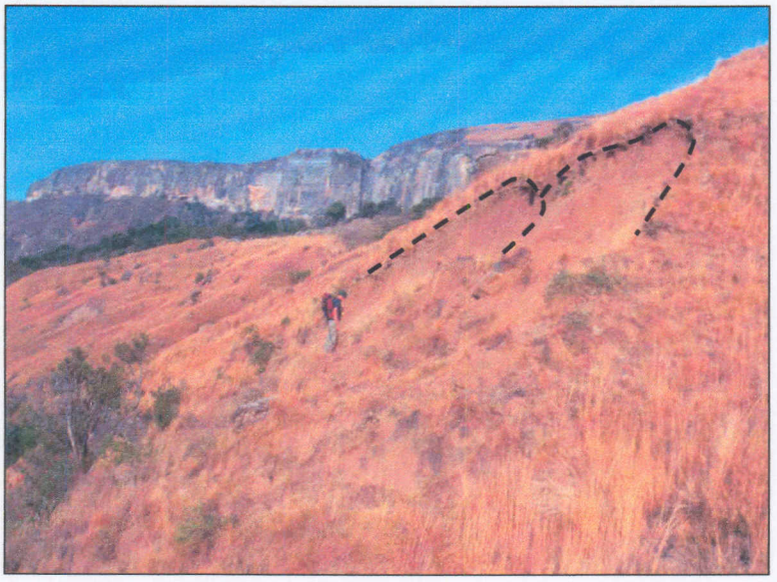

Figure 2.3: Typical arcuate translational landslide scars on the northern facing slopes of the Injisuthi Valley (field worker for scale).

Spatial and temporal distributions of shallow landslides are a factor in landscape evolution of the Injisuthi Valley and are important for the introduction of sediments into streams and rivers of the area. Surficial landslides in the Injisuthi Valley have been triggered by high intensity rainfall events (Wight[1]). Rainfall-induced landslides are, as a rule, relatively shallow (Sidle *et al.*, 1985). As noted in other areas of the world for example in Italy (Borga *et al.*, 1998) and Colombia (Van Westen and Terlien, 1996),

rainfall triggered landslides are ultimately caused by a relative increase in pore pressure of the soils that often develop over a lithological contact between texturally different soil horisons or between the soil and bedrock contact.

Figure 2.4: Road on a paleo-landslide zone in the Injisuthi Valley with economic implications resulting from road slumping.

Garland and Oliver (1993) have investigated landslides triggered by rainfall in KwaZulu-Natal that occurred in the Karoo sequence (in Durban near the eastern coast, South Africa), which is geologically similar to the Injisuthi Valley. It was noted that the rainfall intensity over a three-day period could raise regolith moisture content above a critical level for stability (Garland and Oliver, 1993). High rainfall over a longer period allows pore water pressure to dissipate before it becomes critical, whilst rainfall over short period tend to have greater intensity, resulting in more runoff and less infiltration. Landslides tend to occur towards the end of the wet season and reflect the seasonal build-up of regolith moisture to create suitable mass movement conditions and could be the reason for King's (1982) earlier "two event hypothesis". Water from the first event requires time to soak through the weathered overburden thoroughly before the second rainstorm can trigger a failure. Although this hypothesis has not been tested, Garland and Oliver (1993) established a clear relationship between rainfall and annual landslide frequencies in Durban, KwaZulu-Natal.

2.3.3 Soil cracks

In the Injisuthi Valley, longitudinal soil cracks appear to follow the contours on the foothills of the slopes, especially near the wetlands in clay rich soils. Veder (1981) describes the development of cracks as being caused by local stress conditions that exceed the shear strength of the clay and disrupt the soil cohesion. Water from precipitation enters the cracks, the water content increases and the surrounding soil becomes soft. This process further decreases shear strength. In addition, the swelling process generates new stress conditions and new cracks may develop.

The uppermost soil layer that is most exposed to weathering may lose cohesion as a result of the wetting and drying of soils through cracks (Veder, 1981). In addition, soils undergo chemical processes, such as oxidation and decomposition (Veder, 1981). Zones subjacent to soil cracks are also influenced by the seasonal fluctuation of the ground-water table (pore-water pressure) and changes in temperature (Veder, 1981). According to Veder (1981) these influences, together with gravitational forces and the stress relaxation parallel to the surface, may cause slope movement that reduces shear strength, primarily cohesion, and also the angle of internal friction and may, therefore, cause progressive slope failure.

2.3.4 Terracettes

Terracettes are a microrelief form common to the KwaZulu-Natal Drakensberg's Little Berg (Watson, 1988). Terracettes generally have tread lengths of 0.1-0.5m and risers of 0.05-0.25m high as measured by Boelhouwers (1992) in Gaint's Castle. Terracettes are formed by processes such as soil slippage, soil flow and soil creep. Animal disturbance may be instrumental in triggering the initiating processes or in facilitating their subsequent development (Watson, 1988). Grass tussocks generally bind terracettes, while roots and organic matter binds the topsoil and maintain the miniature scarp. Once terracettes are formed they are subjected to a range of erosional and denudational processes. Terracettes are a general indicator of slope instability.

2.3.5 Soil pipes

Soil pipes in Giant's Castle Game Reserve (the Injisuthi Valley is located in northern corner of this reserve) have two modes of formation. First, soils containing a significant dispersive clay fraction where water percolates through the profile along a zone of greater permeability, thereby removing dispersive clays causing enlarged voids.

Individual grains become dislodged and entrained with the flow, leading to an accelerated system causing tunnels of 0.5m to 0.8m diameter prior to collapse (Garland and Humphrey, 1992). The second type of pipe system is found on scree slopes within the Giant's Castle region and is apparently reliant on loose or very weakly consolidated sediment with a high silt content occurring in conjunction with course scree material (Boelhouwers, 1992). According to Boelhouwers (1992) water infiltrates, but due to the low compaction of the sediment matrix, this is easily entrained by flow and removed from the profile, the pipes tend to be smaller in diameter than those related to dispersion but are also more permanent. Soil pipes carry a significant downslope flow of water and sediment and act as bypasses to soil throughflow. Soil pipes are speed delivery structures to the slope base of whatever inflow they receive, thereby reducing the soil moisture required for landsliding. Soil pipes in the Injisuthi Valley have also been noted to collapse and form gullies.

2.4 Climate

The mean monthly temperatures for Giant's Castle Game Reserve range between 2°C in July and 15°C in January (Schulze, 1981). Asymmetry of incoming radiation on opposite valley sides has a major impact on the temperature and soil moisture conditions and is a prime factor in the development of distinct valley asymmetry in the Little Berg (Boelhouwers, 1988b). The Drakensberg receives the most rainfall during January and February, where the five summer months from November to March account for 70 per cent of the annual rainfall, and the four winter months, from May to August, less than 10 per cent (Tyson *et al.*, 1976). Altitudinal boundaries in rainfall vary between 1000mm in the Little Berg (below 2000m a.s.l.) and up to 1800mm on the Escarpment (2000-3000m a.s.l.) (Tyson *et al.*, 1976). Variations in the rainfall measured at the Giant's Castle Game Reserve weather station (Figure 2.5) (obtained from the South African Weather Bureau) are the closest available approximation of rainfall of the Injisuthi Valley which is located in the northern corner of this reserve.

The amount of rainfall that can infiltrate the soil is influenced by the potential evapotranspiration (PET) of the area. PET is influenced by the characteristics of vegetation, soil properties and aspect (Tyson *et al.*, 1976). Typical seasonal and aspect differences are summarised in Table 2.2.

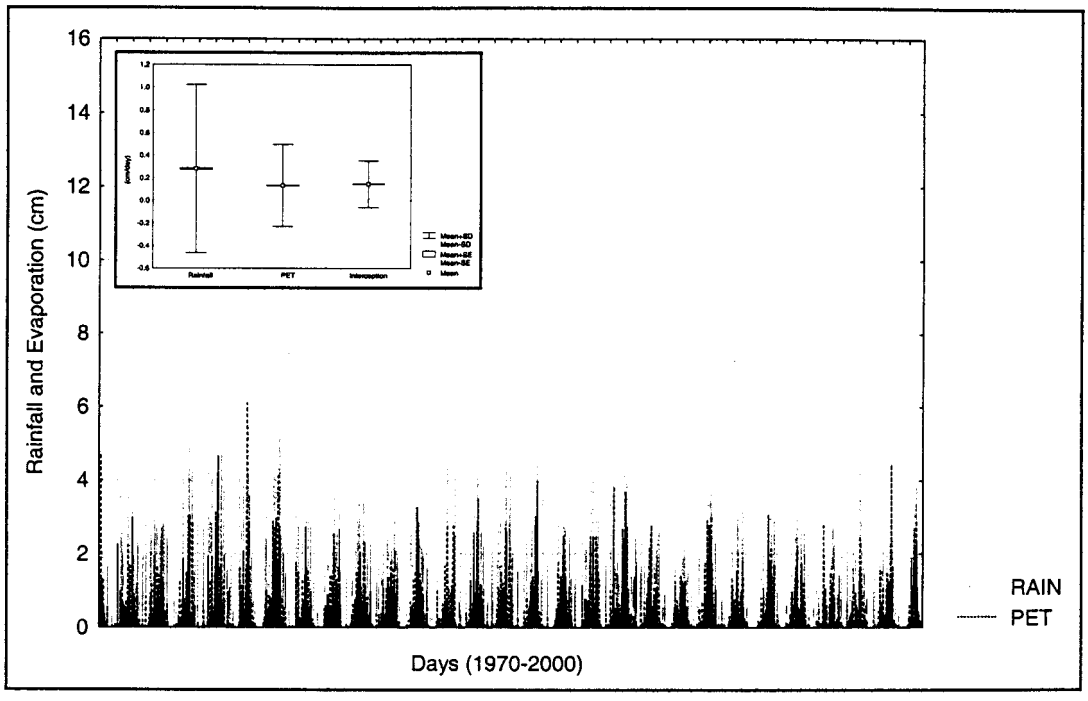

Figure 2.5: Daily rainfall and average PET values for the Giant's Castle Game Reserve (1970-2000). The mean and standard deviation of the rainfall, PET and vegetation interception are shown in the figure inset.

Table 2.2. Average variations in PET (cm) for a typical north and south facing slope in the KwaZulu-Natal Drakensberg (Source: Schulze, 1974 In Tyson *et al.*, 1976).

	North facing slope	South facing slope
Annual	4.01	4.59
Summer	6.15	6.36
Winter	0.84	1.14

Everson *et al.* (1998) measured the average PET for Drakensberg grasslands as approximately 50% of the annual rainfall. According to Tyson *et al.* (1976) PET can be as high as 62% during the wet summer season and decreasing to about 10% in winter. Fluctuations in rainfall and associated PET for the years 1970 to 2000 are summarized in Figure 2.4. PET values were estimated to be approximately 8.6% per month ranging form the highest PET value in January and the lowest in PET July (Appendix 1) based on the work of Tyson *et al.* (1976).

2.5 Vegetation

Three altitudinal zones of vegetation in the KwaZulu-Natal Drakensberg have been identified by Killick (1963) as: Montane (1280-1829m), Subalpine (1829-2865m) and the Alpine (above 2865m) belts. In the subalpine belt grasslands dominated by *Themeda triandra* and various scrubs are common. The Alpine belt consists of heath communities (mainly *Ericas* and *Helichrysum*) while grassland patches are generally broken up by frost action. The Injisuthi Valley Little Berg (Figure 2.2) is situated in the Montane vegetal belt and has been described by O'Connor and Bredenkamp (1997) where *Hyparrhenia hirta* tall grassland is common at altitudes of 1200-1400m a.s.l, while altitudes higher than 1700m a.s.l. comprise *Monocybium ceresiiforme-Tristachya leucothrix* grassland throughout the Drakensberg. In a general description of the dominant grassland species in South Africa, *Themeda triandra* and *Trachypogon spicatus,* are identified as the dominant species for the northern facing and southern facing slopes respectively (O'Connor and Bredenkamp, 1997). Acocks (1975) provides a more specific description for dominant species for the Drakensberg as tufted grasses; *Themeda triandra* usually occurs in open grassland whilst *Trachypogon spicatus* occurs on the more woody southern facing slopes. Major plant community differentiation in the area is usually related to climate (rainfall and temperature) associated with altitude. Along the drainage lines *Podocarpus* species are common, and scattered on the higher altitudes the *Protea* species occur with *Acacias* lower down the valley.

2.6 Chapter summary

Various complex geomorphic processes discussed briefly in this chapter are active in the Injisuthi Valley under the current climatological and ecological environmental conditions. Geomorphic processes are all operating simultaneously on all the hillslopes of the valley and this study will focus on the modelling of processes involved in shallow landsliding. In the Injisuthi Valley there is a mix of relict landforms and contemporary processes. Natural processes are influenced by humans; for example the burning programme, which changes some of the vegetation and soil characteristics (Bijker *et al.*, 2001). Other than soil erosion (for which there is some evidence e.g. pipe-gully system), shallow landsliding appears the dominant geomorphic process in the Injisuthi Valley.

Chapter 3: Fieldwork: methods, results and discussion

A coupled hydrological slope stability model requires fieldwork as a basis for its development. Mulder (1991) identifies primary factors of shallow landsliding as soil density, soil cohesion, soil pore pressure, slope angle and soil angle of internal friction (Table 3.1). Measurement of the primary parameters and additional fieldwork is described in this chapter and includes soil type identification, soil textural analysis, vegetation survey, landslide positioning and landslide classification based on morphometric analysis (Table 3.1).

Table 3.1: Fieldwork parameters used as model inputs. Model inputs derived from literature sources are also based on fieldwork.

Stability factors	Parameter	Model input type		
		Field data		Literature
		Mapping	Constant	
Primary	Soil depth	✔		
	Soil bulk density		✔	
	Soil infiltration capacity	✔		
	Soil moisture at field capacity		✔	
	Soil shear strength		✔	
Secondary	Vegetation cohesion			✔
	Vegetation interception			✔
	Position of landslides	✔		
	Angle of internal friction of soil			✔

Shallow landslide prediction models in a Geographic Information System (GIS) have been developed by authors such as Barling *et al.* (1994), Montgomery and Dietrich (1994) and Borga *et al.* (1998). These studies focus on the primary factors identified by Muller (1991) and include them all as constants in their models with the exception of soil depth (Borga *et al.*, 1998) and saturated infiltration capacity (Barling *et al.*, 1994), which varies (i.e. maps) in the respective models. For the Injisuthi Valley the soil depth and saturated infiltration capacity will be included as maps in a model, while bulk density, shear strength and soil moisture are input constants, derived from the mean value of field measured ranges. Literature estimations for vegetation interception are

based on a vegetation survey and the soil angle of internal friction is derived from soil textural analysis (Table 3.1).

In this chapter the fieldwork procedures and some advantages and disadvantages of alternative methods are noted. Fieldwork equipment and methods were chosen to be simple, yet effective and accurate as the model has scope to be used by field managers for the selection of development areas. Statistical analysis of fieldwork was done in Statistica® (StatSoft Inc., 1995). Where appropriate, the student T-test was used to calculate probable differences between areas and samples within areas, expressed as P values in the text. Samples were considered statistically different at the 95% confidence level ($P<0.05$).

3.1 Fieldwork areas

Contemporary landsliding in the Injisuthi Valley occurs predominantly on the north facing slopes whilst the south facing slopes appear less susceptible to shallow landsliding (*Pers. Obs.*). A north facing site of approximately 3km^2 in the Injisuthi Valley (area S in Figure 3.1) was selected for fieldwork. Some of the fieldwork parameters (bulk density, soil moisture and texture) were also measured in area C (Figure 3.1). The study area (S) was selected to represent typical northern facing slopes in the Injisuthi Valley where the spatial extent of the geological layers, soils and vegetation types were observed to be similar. On all the northern facing slopes in the Injisuthi Valley shallow landslides were also observed to concentrate on steep slopes or in riverbanks, and this is also represented in area S.

Due to soil and vegetation property differences between north and south facing slopes (e.g. Bijker *et al.*, 2001) extrapolation of the model to south facing sites requires additional field investigation. Eastern and western boundaries of area S were chosen to follow natural drainage lines and extend to include all the different lithological layers in the Little Berg (Figure 2.1). Lithologically different layers give rise to different soil properties and it was therefore important to include all the layers. Soil properties can then be generalise within major lithological units (e.g. Tang and Montgomery, 1995).

Area S (Figure 3.1) is representative of a typical northern facing slope in the area within which landslides appear to be concentrated on slopes steeper than 15° and in

riverbanks where river undercutting causes oversteepening. Figure 3.1 indicates the position of field measurement for all the properties summarised in Table 3.1.

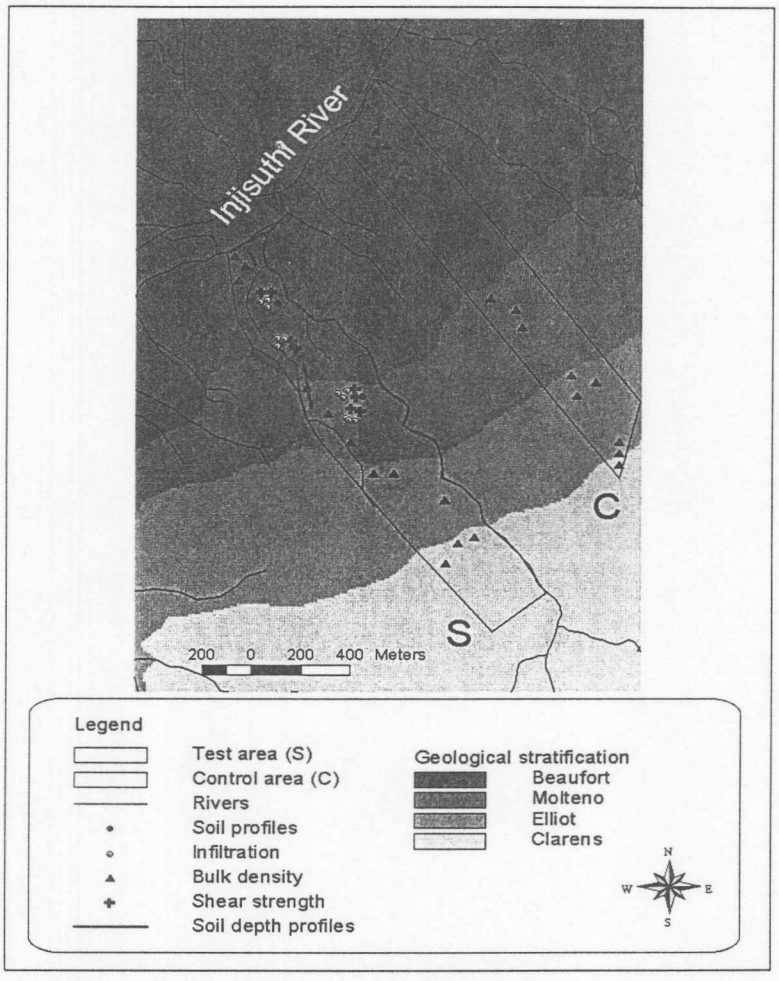

Figure 3.1: Location of sample sites in the test (S) and control (C) areas of the Injisuthi Valley, KwaZulu-Natal Drakensberg.

3.2 Landslide inventory

An inventory of existing landslides in study area S involves their geographical position and then an analysis of their most important characteristics. The location of landslides (section 3.2.1) is required to validate model predictions. Morphometric description (section 3.2.2) is important for the classification of the landslide type and mechanisms involved in sliding.

3.2.1 Landslide positioning

Co-ordinates of landslides in area S were determined with a Trimble Geo Explorer3 Global Positioning System (GPS). This differential[1] GPS is accurate for positioning up to 1m and readings were taken at the centre of each landslide. A global positioning system (GPS) was preferred for landslide location instead of aerial photograph recognition of mass movement features, a method described by Schuster and Krizek (1978). Landslides could not be identified with certainty on the 1:30 000 aerial photographs that were available for the study area. Incorrect landslide locations will result in inaccurate maps. Carrara *et al.* (1992) were able to show that equally experienced researchers compiled different landslide maps in a particular area from the same set of aerial photographs.

The landslide situation on the landscape was noted, particularly the slope angles on which they occur. Of the 98 documented landslides, 37 landslides occurred on hillslopes while 61 were located in riverbank slopes (Figure 3.2). The degree of vegetation recovery (see section 3.5.2) of each landslide scar was noted. Mode of failure was determined using the guidelines of Varnes (1978) which include the extent of displacement of material and characteristics of the sliding plane. In the study area, 13 landslides were classified as rotational and 85 as translational (Appendix 2).

Investigation showed that landslides occur directly above the steepest sections of the hillslope (Figure 3.2). This can be explained by the fact that landslides occur on hillslopes were the soil is deep enough to cause them, as opposed to the very steep slopes which consist of exposed bedrock. Landslides have further been noted to frequently occur in the vicinity of drainage lines. On most of the steep slopes terracettes were found within the landslides and these were identified and classified as cattle steps, having been formed in excess of 40 years ago when this area was used for summer grazing of livestock (Meiklejohn[2]).

[1] A differential GPS consists of the normal hand held GPS and an additional set of antennas that receives co-ordinates from at least five base stations with known locations on the land surface. Base stations communicate their co-ordinate locations via a communication satellite to the second set of antennas, in this way calculating the corrections for the handheld GPS up to 1m.

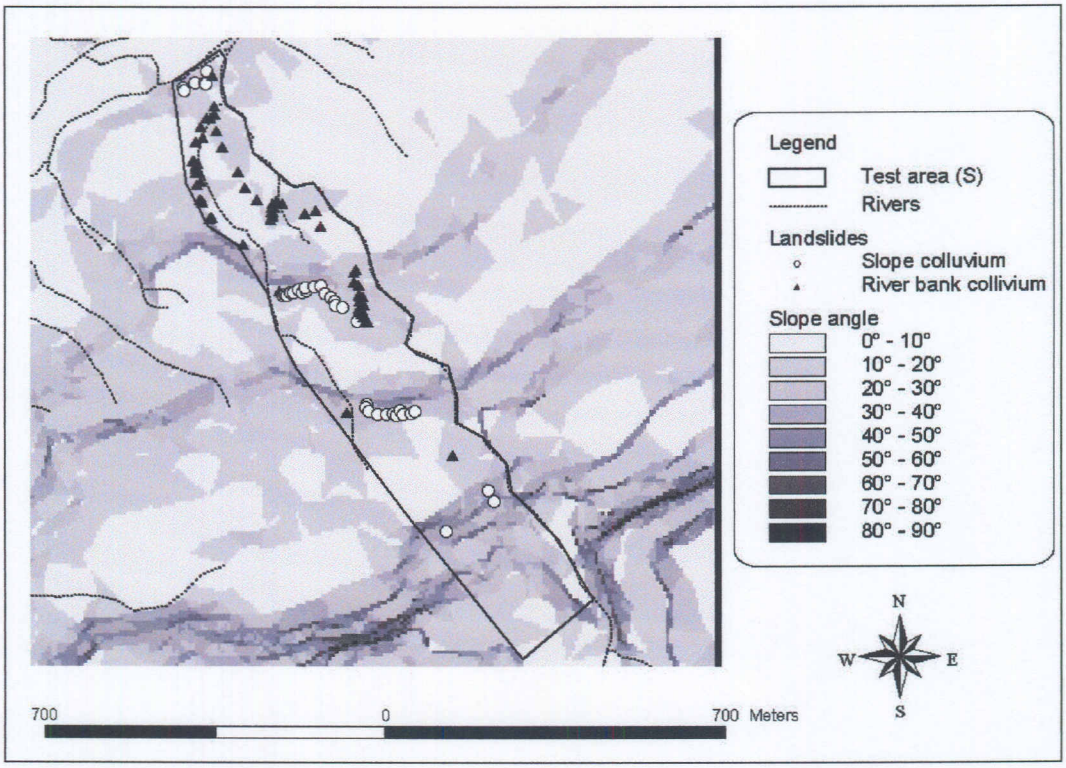

Figure 3.2: ArcView® slope map of area S showing the GPS locations of the 98 landslides.

Figure 3.3: Morphology of the typical translational landslides noted in the riverbanks of study area S (person for scale).

3.2.2 Landslide morphometry

Morphometric parameters in conjunction with the landslide inventory (Appendix 3) facilitated the categorisation of landslides in the study area S in the Injisuthi Valley. Definitions of the measurements that were taken are illustrated in Figure 3.4. Morphometric characteristics of the landslide rupture surface, the length (Lr), width (Wr) and depth (Dr) of 30 hillslope and 30 riverbank slope landslides were measured (Figure 3.2). Only 30 landslides of each category (hillslope or riverbank slope) were randomly selected and used for morphometric comparisons. To determine the conventional depth/length ratio as described by Skempton (1953 cited in Blong, 1973a) only the 30 landslides occurring on soil were used. This was done because the removal of deposits by stream action prevents the use of depth/length ratio calculations for landslides occurring in the 30 landslides occurring in riverbank slope.

Landslides occurring on hillslopes were in generally larger than those noted on the riverbank slopes (Table 3.2); resulting from the confined space for landslides to take place while hillslopes often have a larger spatial extent where landslides can take place. The average maximum (based on Figure 3.4) volume of sediment that is displaced by a landslide event on hillslopes is 70.97m^3 while landslides in riverbanks deposit a average of 52.74m^3 of soil into rivers with each landslide event (Table 3.2). It is important to note that the depth of most of the translational landslides is much deeper than the original shear plane as a result of erosion of the landslide scars, and the area and volume calculations are a maximum estimates.

Average D/L ratio of landslides noted in Table 3.2 can be classified as translational based on the ratios found by Crozier (1973) which vary between 5-8%, and Blong (1973a) between 3-5%. According to Sidle *et al.* (1985), rainfall-induced landslides are, as a rule relatively shallow. Rotational landslides, on the other hand, are characterised by a much larger D/L ratio, for example: 18.2-24.2% noted by Crozier (1973) and 15-27% noted by Blong (1973a). The morphometric analysis thus confirms that landslides in the study area are predominantly translational.

It is evident that landslides on the slopes are slightly larger than landslides occurring in the slopes of riverbanks (Table 3.2). This is a result of the riverbanks having a confined space for landslides to take place as opposed to landslides occurring on hillslopes where large areas of soil are available for sliding. The student T-test was

used to determine the significance of the difference in landslide size based on location (Table 3.3).

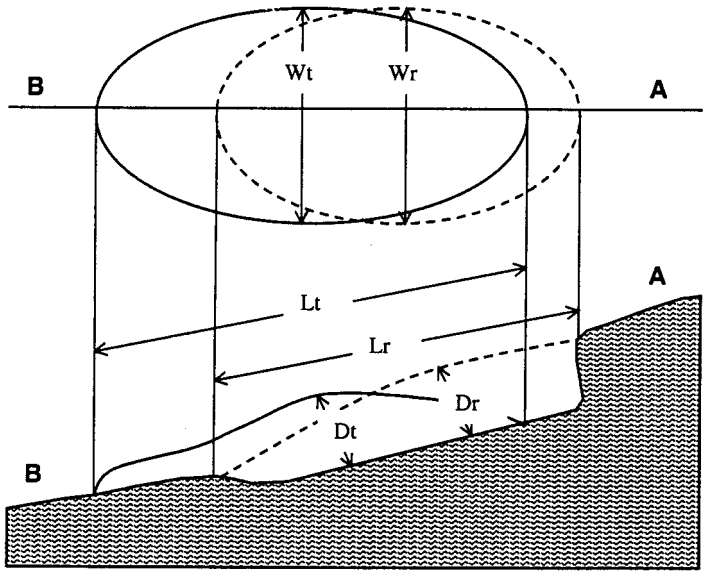

Landslide dimensions:

Lr: the maximum distance from the crown to the toe of the rupture surface.
Wr: the maximum width between the flanks of the landslides, perpendicular to Lr.
Dr: the maximum depth of the rupture surface below he original ground surface measured perpendicular to the plane containing width and length of the rupture surface.
Lt: the maximum distance from the crown to the tip of the landslide.
Wt: maximum breadth of the displaced mass perpendicular to the length Lt.
Dt: the maximum depth of the displaced mass measured perpendicular to the lane containing Wt and Lt.

Figure 3.4: Terminology for the morphometric description of landslides (after Brunsden, 1993).

Table 3.2: Average landslide morphometry (Figure 3.4) measurements for 30 landslides occurring on hillslopes and in riverbanks respectively.

Landslide position	Length (Lr)	Width (Wr)	Depth (Dr)	Dr/Lr ratio	Area m^2 (Lr.Wr)	Volume m^3 (Lr.Wr.Dr)
1. Hillslope	9.92	11.01	0.61	8.31	111.82	70.97
2. Riverbank	7.94	8.62	0.56	8.02	77.75	52.74

Table 3.3 Results of the students t-test for determining the morphological difference of landslides located on hillslopes or in riverbanks.

Morphometry		Mean	Std.Dv	N	P	Difference
1) D/L	Hillslope	0.07	0.02	30	0.11	Not significant
	Riverbank	0.08	0.02			
2) Area	Hillslope	111.82	89.38	30	0.16	Not significant
	Riverbank	77.75	87.94			
3) Volume	Hillslope	87.55	126.09	30	0.18	Not significant
	Riverbank	52.74	68.28			

Evident from Table 3.3 there is that no significant difference in the morphometry of the rupture surfaces of landslides occurring on steep hillslopes or riverbank slopes. The average areas displaced by landslides it is in the vicinity of 10m by 10m, which corresponds to pixel sizes that can be used for the input maps.

A strong positive correlation (*r=0.76*) between the depth and length (Dr/Lr) measurements of the landslides was noted for study area S (Appendix 3). Results indicate that landslide scars tend to increase both in length and depth dimensions simultaneously. Landslide scar interquartile length ranges from 4.40m to 11.05m, while the value for width ranges between 6.20m to13.83m and depth ranges between 0.38m and 0.70m (Appendix 3).

Morphometry measurements give an indication, first of the mechanism of sliding and second of the maximum amount of soil that is displaced by sliding. Retrogressive failures, a phenomenon described by Van Asch *et al.* (1984) and Beckedahl *et al.* (1988) are sometimes associated with translational landslides in study area S and result from the extension of landslide scars from the base to the top, in the direction opposite to the soil movement. Veder (1981) outlines the preconditions for the formation of retrogressive failures, termed progressive failures.

Detailed morphomeric classification of landslides can involve up to 19 numerical attributes of landslides (Blong, 1973b). D/L ratios have been used to validate the classification of landslides as either translational or rotational, and to give an indication of the amount of soil that is displaced in a landslide event (Blong, 1973a; Crozier, 1973). The complexity of classification of mass movement features is illustrated in a

study by Varnes (1958) where 92 landslides were surveyed of which 78 were complex slope failures involving two to three types of slope failures. Further, nomenclature in classification is also a problem that has been frequently addressed in the literature (Varnes, 1978; Beckedahl *et al.*, 1988; Selby, 1993).

3.3 Soils

Soils are the medium in which landslides occur in the Injisuthi Valley. Analysis of the soil with regard to the type, depth, mechanical and hydrological properties are discussed in this section.

3.3.1 Soil types

Two soil profiles were uncovered in study area S and the master horisons identified to determine the soil types present. These profiles corresponded with the soil layers that can be identified in the riverbanks and are therefore considered representative for the area. Various properties, including the depth of each horison, moisture, colour, mottling, consistence, cementation, concretions, presence of rocks, presence of roots, permeability and underlying material was noted in an inventory documented in Appendix 4. Results of this inventory show that the soils in the study area S form a catena that ranges in development between Westleigh, Avalon and Longlands forms depending on the position on the landscape (Van Der Waals[3]). In all three soil forms, the outstanding characteristic is a soft plinthic B horizon, resulting from clay and mineral particles that are leached down from the upper horizons (Figure 3.5). Differences between the soil forms in the study area are that the Longlands soil form has an E-horizon and the Avalon form has a yellow-brown apedal B horizon where the characteristic soft plintic B horizon has not yet fully developed. The Westleigh soil form has no horizon between the orthic A and soft plintic B horizons (Figure 3.5).

In the plinthic B horizon, oxidation of the minerals occurs in the absence of water to leave visible orange coloured iron and smaller black manganese concretions. Because the absence of water is required for the oxidation of these minerals, the depth of the concretions indicates the fluctuations in the water table between dry and wet seasons of the year. In general the water table reaches a height of 0.5m below the soil surface, which forms the border between the sandy upper horizon and the clay-rich plintic B horizon. Depth of the soft plintic B horizon varies between 35cm and 80cm depending on the soil form (Grondklassifikasiewerkgroep, 1991). The two dominant soil horizons

are the orthic A and soft plintic B-horizons and for the remainder of the study reference will be made to these horizons.

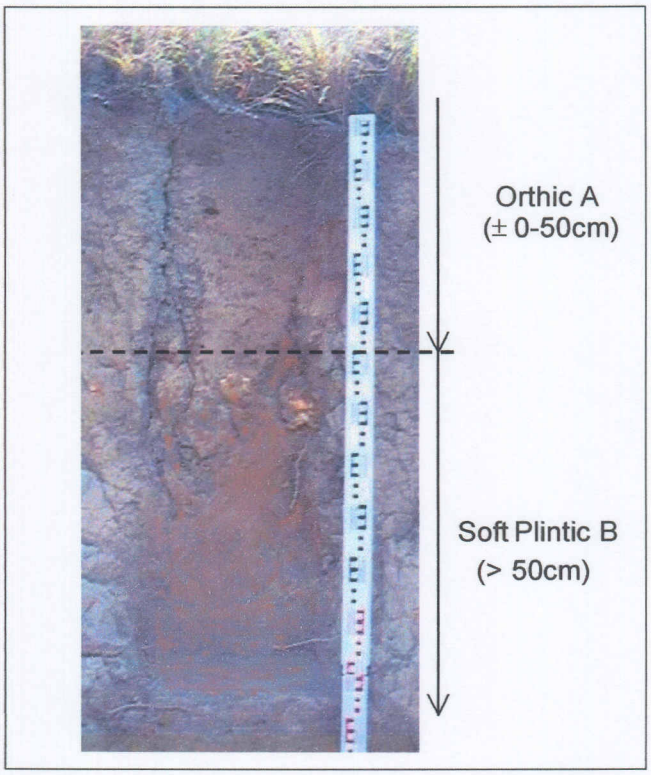

Figure 3.5: Westleigh soil profile showing the characteristic soft plinthic B horison.

Shallow translational landslides occur at an average depth of 0.5m (Table 3.2). At this depth the interface between the orthic A and plintic B horizons occurs. The soft plintic B horizon is in general more clay rich and water concentration at the interface between the orthic A and plintic B horizons results in localised increase in pore water pressure, increasing the likelihood of landsliding with the soft plintic B horizon acting as the shear plane. This is contradictory to the findings of Sumner (1993) that landslides in the KZN Drakensberg occur at the interface between soil and subsurface geology.

3.3.2. Soil depth

Soil depth in study area S was determined with a dynamic cone penetrometer (DCP). Soil depth was ascertained along three profiles, where distances between natural breaks in the slope were measured and at every break the average slope angle was measured with an abney level. A total of 31 points were measured for slope angle and soil depth and the details of the survey are in Appendix 5. The maximum rod length of

the DCP was 2m but often deeper soil (>2m) was noted at the riverbanks. The maximum slope angle included in the measurements was 45° (Table 3.4).

Table 3.4: Slope angle ranges and associated average soil depth (n=31).

Slope angle range (°)	Average soil depth (m)	Sample points (n)
0-5	2.00	3
5-10	1.40	3
10-15	2.00	1
15-20	2.00	2
20-25	1.09	8
25-30	0.42	2
30-35	1.20	3
35-40	0.59	7
40-45	0.71	2

Correlation between soil depth and slope angle was undertaken using the average slope angle and soil depth ranges (Table x) in Statistica® (Statsoft Inc., 1995). Figure 3.6 shows a strong negative correlation (*r=–0.6310; n=31)* between soil depth and slope angle which implies that with an increase in slope angle there is a decrease in soil depth. It was noted in the field that slopes steeper than 45° seldom contain enough soil for landslides to take place.

A map of the soil depth is constructed as model input based on the values of the Table 3.6 and the correlation in Figure 3.6. Assuming a linear relationship, soil depths were assigned to slope angles based on the regression correlation relationship and the specific values for each slope category is summarised in Appendix 5. Soil depth of the study area ranged between 0.1cm and 370cm with a computed average of 222cm and 95% of the area contains soil that are 22.2 ± 9.1m deep (Figure 3.7).

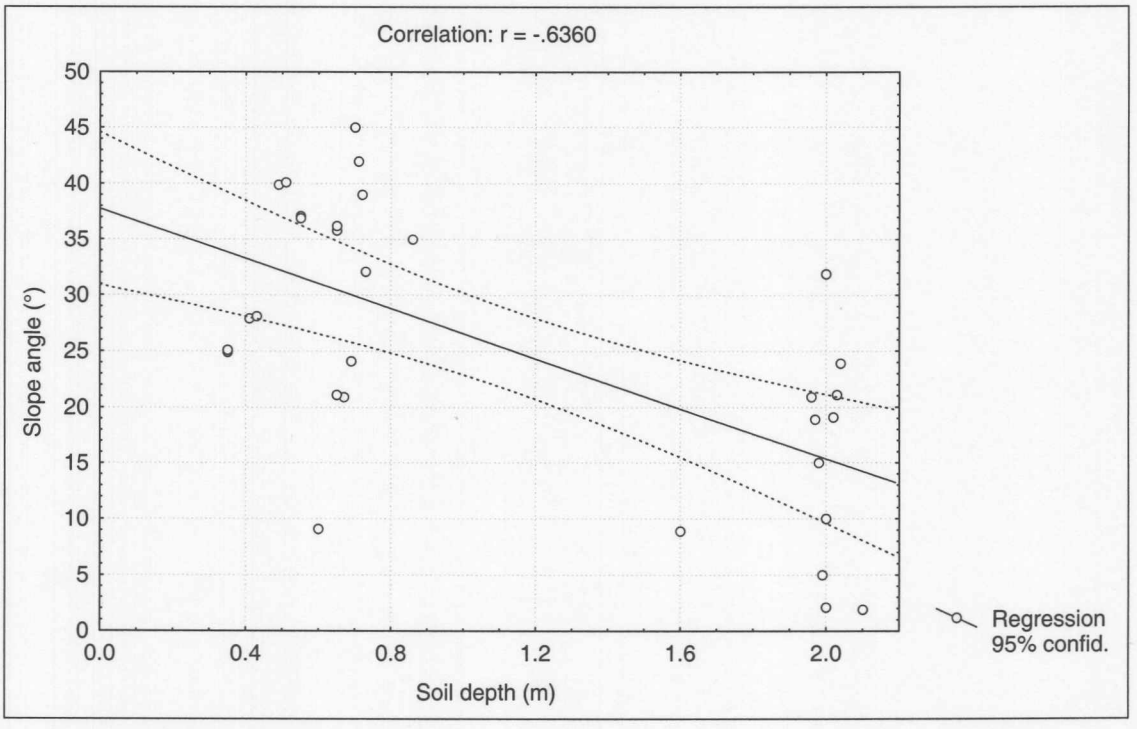

Figure 3.6: Linear regression and correlation of soil depth and slope gradient (n=31, some points overlap).

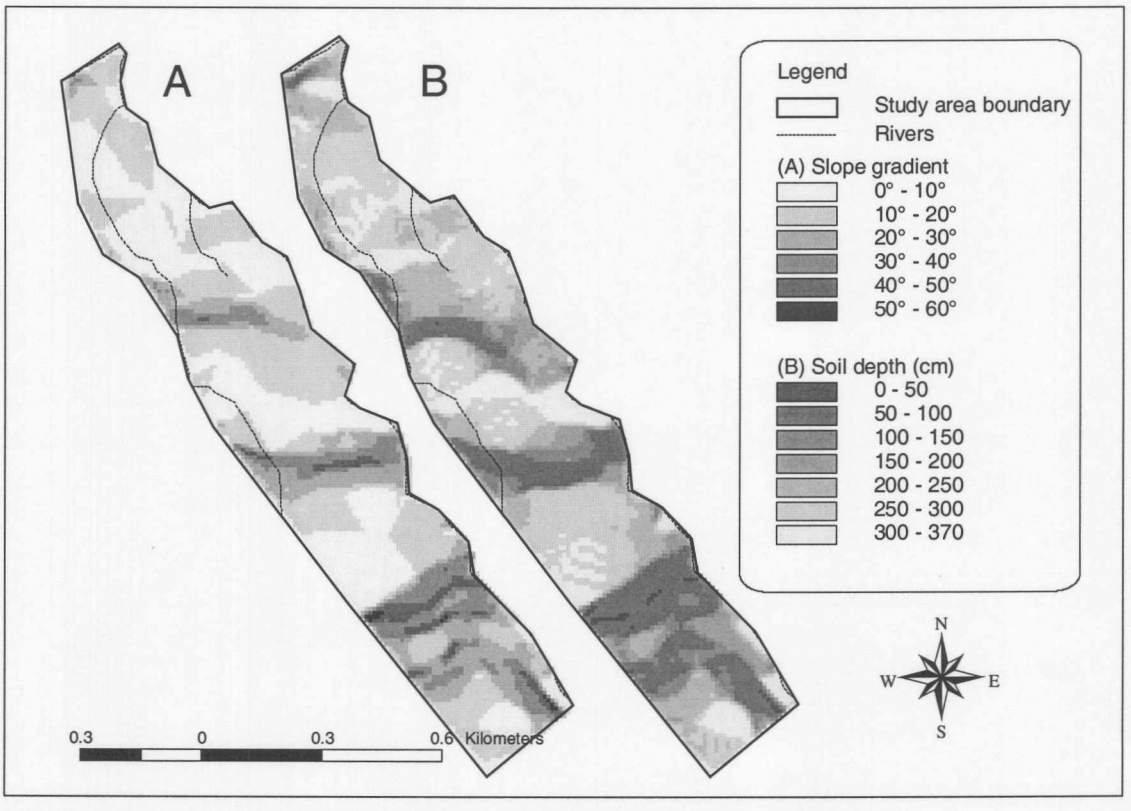

Figure 3.7: Slope angle (A) and soil depth (B) maps of study area S.

Slopes steeper than 50° contain soils of 0.1cm deep in which landslides do not take place. The significance of soil depth in shallow landslide modelling is related to the amount of water that can infiltrate and percolate through the soil profile. Deeper soil profiles can absorb more water, whilst shallow soils saturate faster during a rainfall event and are subsequently more prone to slope instability. Soils deeper than 2m are not prone to landsliding as the shear plane for sliding occurs at the interface between the orthic A and more clay-rich soft plintic B horizon which occurs approximately 50cm below the soil surface (section 3.3.1).

3.3.3 Soil physical properties

The soil physical properties analysed with respect to modelling (Table 3.1) include the bulk density and soil texture from which the angle of internal friction of the soil will be derived. Texture also gives an indication of the hydraulic properties of soils in the study area.

3.3.3.1 Soil texture

Soil texture plays an important role in the moisture balance of soils (Finlayson and Statham, 1980); clay soils have the capacity to hold more water than sandy soils. Twelve soils samples from study area S were analysed for texture. Oven dried soil was mechanically disaggregated with a mortar and pestle and sieved for 10 minutes at 60 Hertz to separate the gravel (>2.0mm), sand (2.0-0.05mm) and silt plus clay (>0.05mm) fractions. In order to separate the grain size proportions for the silt (0.05-0.002mm) and clay (<0.002mm) fractions, the pipette method of dispersed particle settling under Stokes' Law was used (Briggs, 1977) (Appendix 6).

Results from the texture analysis show that samples taken at a depth of 0.5m (D0,5) are predominantly sandy loam, whilst samples taken at 1m (D1) are classified mostly as clay loam soils (Figure 3.8). The D1 samples are supported by the samples taken at the soil profile (P) which are predominantly sandy silt loam. The increase in clay content lower down the soil profile corresponds with observations by Garland and Humprey (1992). Westleigh soil form (Section 3.4.1) comprises clay rich lower horisons. Soil textures on the upper 20cm of soils (S and C, in Figure 3.8) both have a sandy loam texture.

Differences in soil texture (sand, silt and clay components) between the sample sites were analysed using the multivariate analysis technique of Multi-dimensional Scaling (MDS) in PRIMER v4.0 1994 (Clarke and Warwick, 1994). To give an indication of how the changes in texture related to the depth of the soil a comparison was made between sites S and C (top 20cm of soil) with D1+P (1m depth of soil). The soil texture components were marked with a subscript 1 for sand, 2 for silt and 3 for clay. Figure 3.9 is the result of the MDS. The distance between points is an indication of the degree of similarity between the soil samples. Evident from Figure 3.9 is that the the clay contents of the top soil samples (S_3 and C_3) are more similar to each other than to the 1m deep sample (D_3). The sand and silt contents of the Test area (S_1, S_2), Control area (C_1, C_2) and the deep sample (D_1, D_2) are similar to each other.

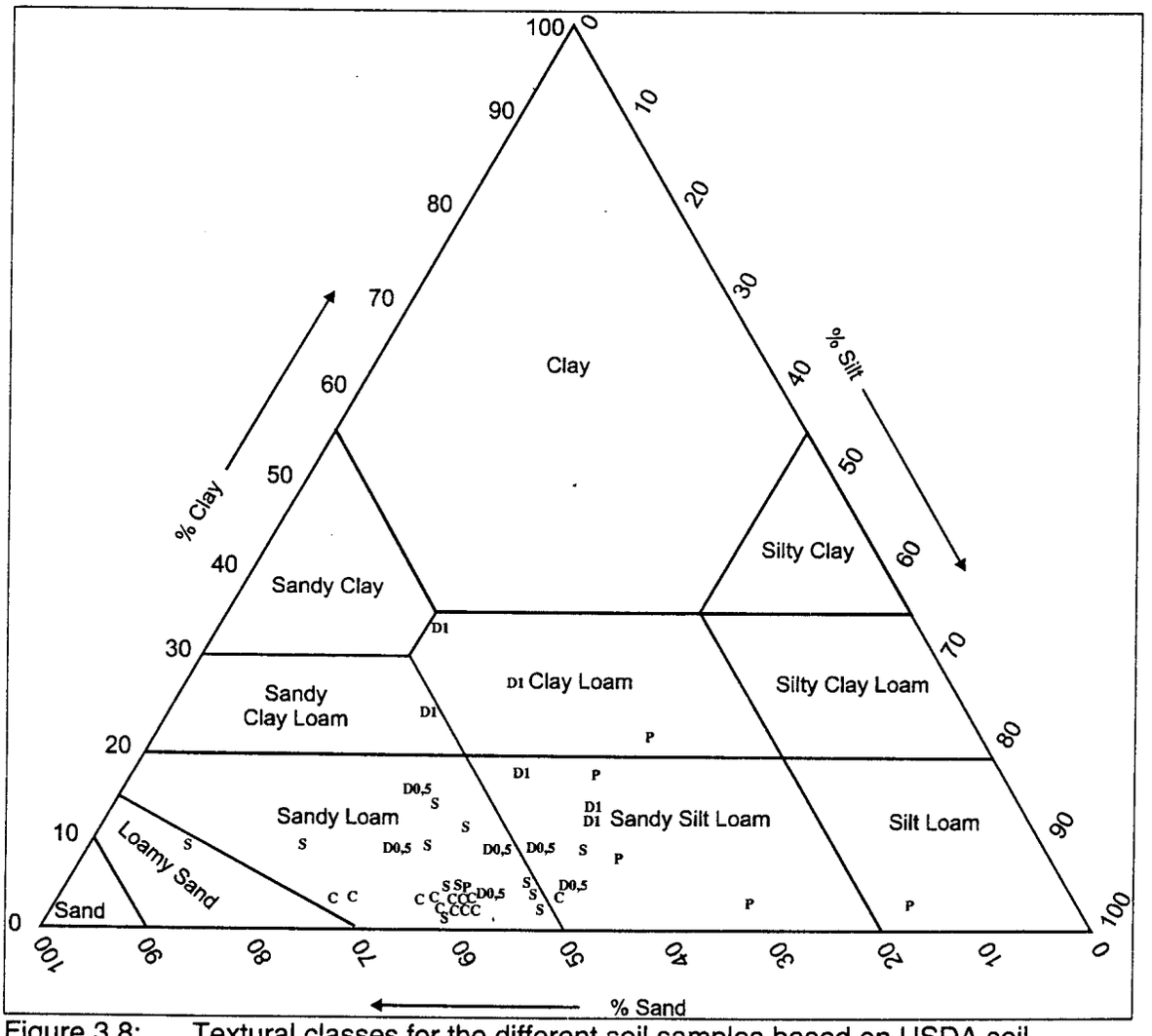

Figure 3.8: Textural classes for the different soil samples based on USDA soil classification (S = Test area, C = Control area, P = Soil profiles, D = Depth at 0,5m or 1m of soils).

An analysis of similarity (ANOSIM, Clarke, 1993) was used to establish the significance of differences between sample areas S, C and D1+P as a whole, including the sand, silt and clay components. The ANOSIM is a non-parametric permutation procedure applied to rank similarity matrices underlying sample ordinations in which a significant global R-statistic is calculated. Global R values range between 0 and 1. A value close to 1 indicates distinct differences between the groups concerned and the similarity within each group is higher; a value near 0 indicate greater similarity between and within each cluster. Results of the global R-value show that the three groups are very similar (Figure 3.9). The topsoil surfaces, areas S and C were more similar to each other (*R=-0.259*) than comparisons with the deeper soils, where sites S and D1+P (*R=-0.296*) and sites C and D1+P (*R=-0.296*) differ more in soil texture. The similarity between groups is explained by Figure 3.9 where the clay component is the biggest contributor to dissimilarity between and within each group. The sand and slit components show a high similarity between and within all the groups.

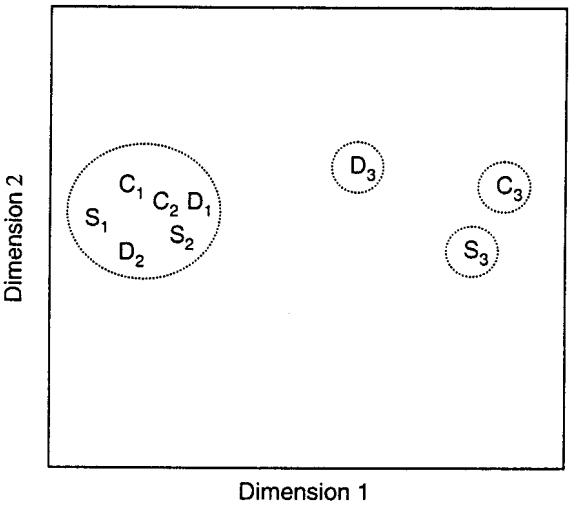

Figure 3.9: Results from the non-parametric multidimensional scaling (MDS) analysis.

The observation that areas S and C show greater similarity to each other than to the soil texture at 1m depth, indicated that the soils are horizontally more homogeneous in texture and vertically more heterogeneous in texture. The findings support textural differences in the orthic A horizon and lower, more clay rich soft plintic B horizon as noted in section 3.3.1.

3.3.3.2 Bulk density

A hammer-driven core sampler was used to collect twelve bulk density samples on the soil surface in the study areas S and C respectively (Figure 3.1) and at a depth of 1m below the soil surface in area S, referred to here as area D. Tan (1996) suggest sample weights between 125-500g for bulk density analysis and the samples collected for areas S and C fell approximately within this range with weights between 144.1g and 611.5g. The dry bulk density for each core sample was calculated as the mass (g) of the oven dried sample in the volume (cm^3) of the soil including air and water (Campbell and Henshall, 1991). Sampling at depths below 14cm proved problematic but was attempted at 12 sites occurring in the riverbanks in study area S, referred to here as sample set D.

Average bulk density for area S (Figure 3.1) was 0.7±0.1g/cm^3, area C was 1.3±1.1 g/cm^3 and at a depth of 1m, area D, it was 1.1 ±0.5 g/cm^3 (see Appendix 7 for survey details). Although it is expected that the test area (S) and control (C) have similar bulk density values, because they are both north facing with similar soils, a t-test result show that the areas differ significantly ($P=2.6x10^{-2}$) at the 95% confidence level (Appendix 7). The lower bulk density of area S compared to area C can be explained by the higher organic content of area S having a higher volume of voids in the soil. Further, the control area C has recently been burned, exposing the soil surface and making the soil more desiccated compared to area S, where vegetal material covers the soil and maintains soil moisture. At soil depths of 1m below the soil surface of area S a higher bulk density was measured, and this can be explained by the soil being more clay rich and compact at these depths.

The values obtained for bulk density correlate with findings of Little *et al.* (1998) who measured bulk density values in KwaZulu-Natal ranging between 0.9-1.4g/cm^3 for soils varying in clay content between 3-64%. Everson *et al.* (1998) measured average bulk density values of 0.8 g/cm^3 also in KwaZulu-Natal. Briggs (1977) suggests guidelines for bulk density values as low as 0.4g/cm^3 for soils with high organic matter but most other mineral soil range between 1.0 and 2.0g/cm^3.

Although there is a significant difference between the two north facing sites S and C (Figure 3.1) the average bulk density value of 1.0±0.3g/cm^3, was used as a constant in

the model (converted to 1.0 x 10^{-4}KN/cm^3) (Table 3.1). Testing the model's sensitivity to this parameter is discussed later.

3.3.3.3 Angle of internal friction

The angle of internal friction (ϕ) of soil is the angle at which the soil will automatically start sliding regardless of any external triggering factors. This can be estimated in the field by the relationship between soil angle of internal friction and percentage clay content of the soil (Figure 3.10) (Gardiner and Dackombe, 1983). In section 3.3.3.1 texture analysis of the soil are described (Appendix 7) and the average clay content for the soils in the study area (S, Figure 3.1) is 2.4%. Low clay fraction results in steeper angles of internal friction and for the study area this range lies between 28°-34° (Figure 3.10).

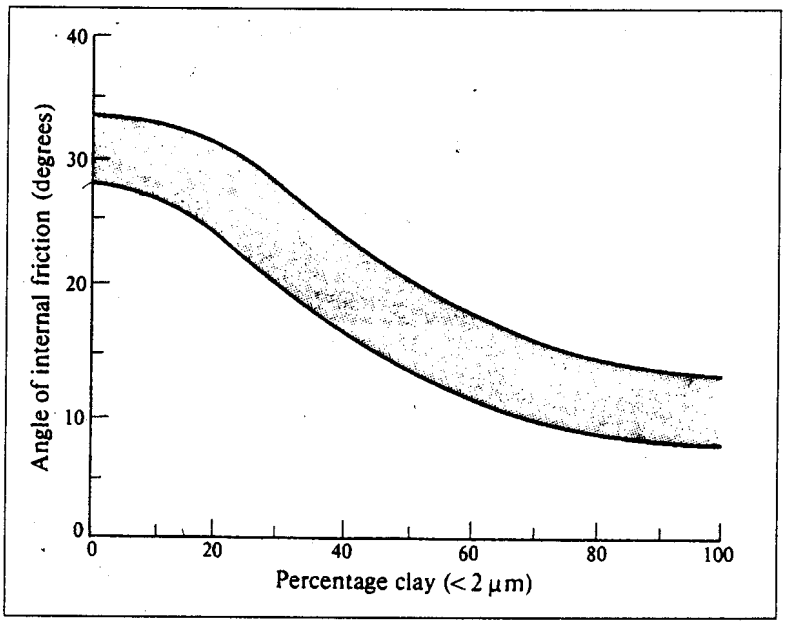

Figure 3.10: Relationship between soil angle of internal friction and percentage clay content (source Gardiner and Dackombe, 1983).

The average for the range in angle of internal friction, namely ϕ=31° will be used in the model as a constant (Table 3.1). Substituting mean values for the ϕ range is a commonly used method in slope stability analysis e.g. Borga *et al.* (1998) used ϕ=35° where a range between 33° and 38° was suggested. For slope stability analysis this implies that all the slopes steeper than 31° are inherently unstable ($\tan\alpha<\tan\phi$). Important to note here is that the clay content of soils lower down the profile is on

average 15.4% (Appendix 7) and these soils will have a lower angle of internal friction. The models sensitivity for the bulk density constant will be tested later.

3.3.4 Soil hydrological properties

Soil hydrological properties assessed to form model inputs include the soil moisture and saturated infiltration capacity (Table 3.1).

3.3.4.1 Soil moisture

The two soil parameters of moisture and density are closely connected; an increase in moisture content will naturally cause a decrease in the dry weight density as water molecules will take the place of the cohesion forces of the soil particles, resulting in less dense soil (Briggs, 1977). Soil samples (Figure 3.1) were weighed, dried in an oven at 105°C for 48 hours, reweighed and the moisture content calculated as a percentage of the dry weight (Briggs, 1977). Results are summarised in Figure 3.11 and details are in Appendix 8. The moisture ranges are similar to the work of Little *et al.* (1998) where soil water content determinations in KwaZulu-Natal values ranged from 14%-54%.

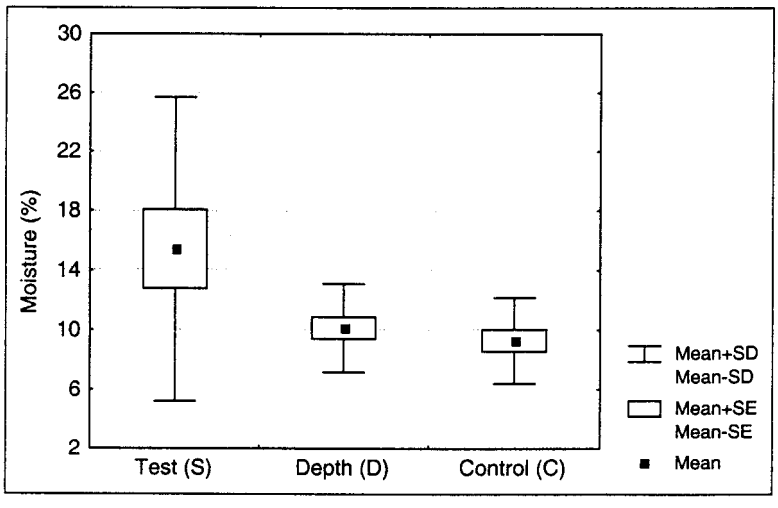

Figure 3.11: Mean, standard deviation and standard error of soil moisture content variations as measured on 23 June 2000.

Soil moisture for area S shows a higher variability than area C and the soils taken at a depth of 0.5m and 1m. Area C has recently been burned and conditions under which soil samples were taken are fairly homogenous, resulting in less variation between readings. In area S there are varying degrees of vegetation cover resulting in different

soil moisture contents. The highest moisture content measured in area S was 43% and this sample site was in a shaded area near the river. This site gives an indication of the maximum amount of water that can be contained in the soil profile. Water content may, however, increase at the plintic B horizon which is a more impermeable soil layer in comparison the upper orthic A horizon.

The landslide prediction model constructed in this study will be based on the work of Montgomery and Dietrich (1994) and Borga *et al.* (1998) where the percolation of water through the soil profile is an important determinant in the temporal prediction of landslides. Soil moisture minimum, maximum and field capacity defines the quantitative boundaries of water movement through the soil. Soil samples were collected one day after it rained, and therefore the soil moisture content measured is slightly more than the field capacity of the soils. The soil moisture at field capacity is a term used to define the maximum amount of water in the soil left after gravitation removed all the access water (Briggs, 1977).

Minimum soil moisture for the purpose of this study was inserted into the model at 4%, only 1% lower than the lowest moisture measured from samples taken in the dry winter. Soil moisture at field capacity defines the amount of water left in the soil a few days after it stopped raining (Briggs, 1977). The average soil moisture was measured as 15.4% (Section 3.3.4.1). Soil samples were taken one day after it rained and to compensate for this an estimation of 10% moisture at field capacity was inserted in the model. The highest moisture content measured in the area S was 43% which was located in a shaded area near the river in saturated soils. This site is the only measurement that could give an indication of the maximum water in the soil profile, and the maximum moisture content is inserted as a constant of 43% in the model (Table 3.1). This maximum correlates with the work of Everson *et al.* (1998) in the Drakensberg who found the maximum moisture content varying between 43-50% depending on the season.

3.3.4.2 Infiltration capacity

Another important factor in determining the soil moisture, is the infiltration capacity of soils. Infiltration capacity can be defined as the maximum rate at which a given soil can absorb rain as it falls (Horton, 1933). In the absence of a capillary pressure gradient, for example under saturated conditions, the infiltration rate of the water into the soil

reaches a stable rate termed the saturated hydraulic conductivity (Ks). In many infiltration equations Ks equals the steady state infiltration rate established in the course of a rainfall event. Ks, in this study, was measured using the inverted bore hole method (Finlayson and Statham, 1980). Three measurements at four locations (n=12) in area S were used (Figure 3.1).

The inverted bore hole method was chosen, first because a cone is easy to obtain for end users of the model. Second, the alternative to the cone is a rainfall simulator which apart from being a specialised piece of equipment, has been proven to be effective in cultivated land with a uniform soil crust, but not in grasslands where irregular surface crusting occurs, such as the slopes of the Injisuthi Valley (Morin and Benyamini, 1988 cited in Morin and Kosovsky, 1995). Further, rainfall simulators have a constant rainfall intensity seldom found under natural conditions, where rainstorms consist of a set of brief segments that vary in rainfall intensities. The fluctuation of these intensities is the main reason for the dramatic reduction of runoff by smaller increases in surface storage (Morin and Kosovsky, 1995). A uniform rainfall intensity masks the storage phenomenom of soil as described by Morin and Benyamini (1988).

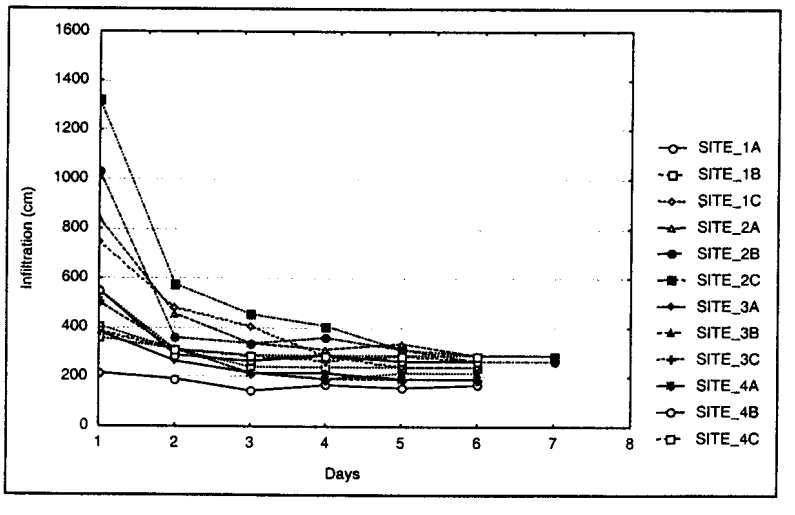

Figure 3.12: Infiltration capacity of the sandy loam soils in area S.

Infiltration capacity of the study area ranges between 156 and 288cm/day (Figure 3.12). Infiltration capacity is correlated to slope angle and to soil texture (Briggs, 1977). It is expected that less infiltration will take place on steeper slopes, as a result of higher runoff (Bonsu, 1992). A slope angle of 15° was chosen as the cut-off point because at these angles landslides start taking place. The soil infiltration capacity is

summarised two main zones, the first on slopes ranging between 15° and 80° as 156cm/day and on slopes ranging between 0° and 15° as 288cm/day.

Infiltration rates of the soils lower down the soil profile have been measured, using a cylinder infiltrometer at a depth of 1.2m as being five times lower than the top soil for the Kamberg Nature Reserve in the KwaZulu-Natal Drakensberg (Garland and Humphrey,1992). This lower infiltration capacity can be explained by the 33-43% increase in the clay with soil depth. Morgan *et al.* (1998) proposes an infiltration range between 0.96 - 91.2 cm/day for clay loam soils (Figure 3.8) found in the lower sections of the soil profiles in the Injisuthi Valley. In this study the infiltration capacity of soils below the surface was not measured, however from the texture analysis (section 3.3.3.1) it is evident that there is a clear increase in clay content with depth for the soils of the study area. To accommodate differences in the infiltration capacities of the orthic A and soft plintic B horizons, a second set of maps were constructed for the B horizon. Based on the work of Garland and Humphrey (1992) infiltration capacities of 31.5cm/day were assigned to slopes with angles of 15° to 80° and 57.6cm/day for slopes ranging between 0° and 15° based on the assumption that the infiltration values are 5 times lower than the upper orthic A horizon.

A complex interrelationship exists between infiltration and aspects of the biotic and abiotic environment. This necessitates extensive replication of measurements and in this study the replication of three measurements at four sites in a study area was sufficient to give similar infiltration measurements, shown in Figure 3.12. Factors that have a major influence of the infiltration values area the surface crusting of soils (Morin and Kosovksy, 1995), the land-use type, the ability of the vegetation to produce a deep litter layer Tricker (1981), while the slope angle is of less, although significant importance. It is generally accepted that steep slopes encourage surface runoff, causing a negative relationship between infiltration and slope angle (Tricker, 1981; Ward and Robinson, 1990; Bonsu, 1992). Poesen (1984) however, found a positive relation between slope and infiltration rate for soils that are susceptible to surface sealing. Surface sealing occurs when soil particles dispersed through the impacting force of raindrops tend to block soil pores (Bonsu, 1992). Apart from slope angle, the seasonal variations in soil moisture conditions may influence the infiltration rate of soils.

3.3.5 Soil mechanical properties

Soil cohesion is a mechanical soil property determined by measuring the shear strength of the soil (Table 3.1).

3.3.5.1 Shear strength

A Pilcon hånd shear vane was used to measure the shear strength of the upper 5cm of (Serota and Jangle, 1972). Four sites in study area S representing the different geological formations (Figure 3.1) were selected to give an indication of the spatial variability of shear strength of the soil. (Taking shear strength measurements below the soil surface at a depth of 0.5 m (at the landslide shear plane) was attempted, however, the soil was too hard for the instrument to penetrate). Average findings for study area S are summarised in Figure 3.13 (n=58) (Appendix 9).

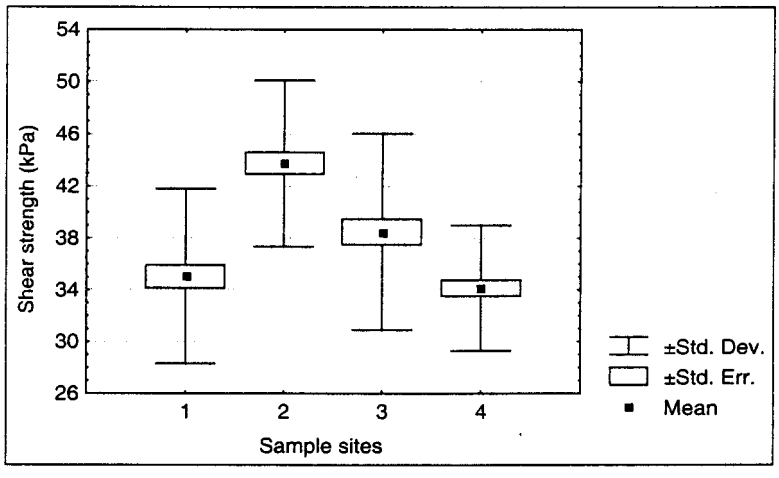

Figure 3.13: Shear strength measurements, the average, standard error and standard deviation for four locations in area S (n=58).

The spatial variability in the shear strength (Figure 3.13) is greater within the geological formations, than between the different formations. The variation can be explained by differences in the soil crusts (top 5cm) locally. Differences in shear strength between sites in the study area were assessed using the students T-test (Table 3.5).

Table 3.5: T-test results for determining differences in the shear strength readings for area S.

Sample comparison	P-value	Difference
1 and 2	0.000000	***
1 and 3	0.012424	**
1 and 4	0.447497	NS
2 and 3	0.000204	***
2 and 4	0.000000	***
3 and 4	0.000438	***
Not significant: NS Significance levels: * 90% ** 95% *** 99%		

Shear strength in area S had an average value of 38±4kPa measured for all four sites. The central tendency and variability of the 58 readings taken at four locations in area S is summarised in Figure 3.13. Only samples 1 and 4 (within area S) do not differ significantly (*P=0.447*) from each other (Table 3.5). Comparing the intra-sample variations reveals that at the 95% confidence level for sites 2a and 2b (*P=0.967*) and sites 3a and 3b (*P=0.526*) differ significantly. This is not the case for sites 1a and 1b (*P=0.012*) nor for sites 4a en 4b (*P=0.308*), which explains why sites 1 and 4 do not differ significantly.

The shear strength value inserted as a constant in the model (Table 3.1) is based on the average soil cohesion in area S (N=240) and is 38kPa (3.8×10^{-7} kN/cm^2). Shear strength measurements are considerably higher than those measured in Giant's Castle by Bijker *et al.* (2001) ranging between 1.46-2.89 kPa, and Terlien (1998) who measured 1.8kPa. According to Mulder (1991) grassland vegetation roots extending down to 20 to 30 cm also increases the soil cohesion considerably up to 2.0×10^{-6} kN/cm^2 and the cohesion measures for the study area seem to correspond with those of Mulder (1991). The models sensitivity to the measured range and model input constant will be tested as described in Chapter 5.

3.4 Vegetation

3.4.1 Vegetation survey

Although vegetation data is not a required input for a landslide prediction model (Table 3.1) knowledge on the local vegetation is important to estimate the cohesion and interception values. A vegetation survey was conducted in area S using the Braun-Blanquet technique (Kent and Coker, 1996). Nine potentially different homogenous vegetation units were identified on aerial photographs based on ground rockiness, plant types and altitude. Within the nine units, 3 quadrates of $16m^2$ each were placed 10m apart, giving a survey of 27 quadrats for the study area in total. A quadrate size of $16m^2$ was chosen, as it is a more comprehensive survey technique than the minimum size quadrate of $4m^2$ accepted for grasslands (Kent and Coker, 1996; Fletcher, 1997). For each quadrate the plant species were identified and their percentage cover estimated using the classification presented in Table 3.6.

Table 3.6: The Braun Blanquet vegetation cover scale.

Value	Braun Blanquet cover abundance value
+	A single individual, with a low basal coverage.
r	Present but not abundant, coverage of less than 5%
a	6-25%
b	26-75%
c	>76%

Species coverage data were numerically classified using Two Way Indicator Species Analysis, TWINSPAN (Hill, 1979). Quadrates were numerically grouped into classes based of their floristic composition. Table 3.7 illustrates the result of the TWINSPAN classification; in this table the columns refer to quadrats and the rows contain the species. The two lowest blocks in Table 3.7 refer to the dominant vegetation communities present. *Themeda triandra* dominates the first community (common on all the northern facing slopes in the Drakensberg) as well as 2 spots of wetland communities dominated by *Gunnera perpensa*. Spatial locations of the wetland areas are restricted to two small flat areas adjacent to convex slopes where water can concentrate in the landscape. A major determinant of the location of the wetlands is the site-specific topography.

Table 3.7: TWINSPAN vegetation species list showing two distinct plant communities at the base of the table.

Unique releve nr.	1 2 3 4 5 6 7 8 9 1 0	1 1 1 1 1 1 1 1 1 2 1 2 3 4 5 6 7 8 9 0	2 2 2 2 1 2 3 4	2 2 2 5 6 7	2 2	Species reference
Tristachya leucothrix	+					
Helichrysum pilosellum	r +					Helichrysum pilosellum (L.f.) Less.
Watsonia pulchra	r					Watsonia pulchra N.E.Br. ex Goldblatt
Setari sphace v. sphac	r					Setaria sphacelata (Schumach.)
Eragrostis curvula	a		+			Eragrostis curvula (Schrad.) Nees
Helictotrich hirtulum	r					Helictotrichon hirtulum (Steud.) Schweick.
Eragrostis racemosa	r					Eragrostis racemosa (Thunb.) Steud.
Helichrysum acutatum	+ + R + r +			r		Helichrysum acutatum DC.
Merxmuellera disticha	r					Merxmuellera disticha (Nees) Conert
Valeriana capensis	r					
Chlorophytum cooperi	r					Chlorophytum cooperi (Baker) Nordal
Eriospermum cooperi	r					
Gnidia kraussiana	r +					
Eragrostis capensis	+ r					Eragrostis capensis (Thunb.) Trin.
Melinis nerviglumis	r + +					Melinis nerviglumis (Franch.) Zizka
Panicum natalense	+ + + + r	+			a	Panicum natalense Hochst.
Crassula alba v. alba	+ + + +		r r r			Crassula alba Forssk. var. alba
Hypoxis rigidula		r				
Oxalis smithiana		r				Oxalis smithiana Eckl. & Zeyh.
Rhus discolor		+				Rhus discolor E.Mey. ex Sond.
Lotononis lotononoides		r				Lotononis lotononoides (Scott-Elliot) B.-E.van Wyk
Cusson panicu s. panic		R				Cussonia paniculata Eckl. & Zeyh. ssp. Paniculata
Gazania krebsiana		R				
Monocymbium ceresiifor		a				Monocymbium ceresiiforme (Nees) Stapf
Rhus montana		R				Rhus montana Diels
Syncolostemo macranthu		R				Syncolostemon macranthus (G rke) M.Ashby
Zantedeschia aethiopic		R				Zantedeschia aethiopica (L.) Spreng.
Leonotis ocymifolia		R	r			
Lotononis dichiloides		r				Lotononis dichiloides Sond.
Protea roupelliae		+				
Aponogeton junceus	r	+				
Phylica paniculata		r +				Phylica paniculata Willd.
Argyrolobium speciosum		r +				Argyrolobium speciosum Eckl. & Zeyh.
Trachypogon spicatus		b a				Trachypogon spicatus (L.f.) Kuntze
Schistosteph hippiifol		+ + r				Schistostephium hippiifolium (DC.) Hutch.
Watsonia meriana	r	r				Watsonia meriana (L.) Mill.
Protea caffra s. caffr	r +	+ r				Protea caffra Meisn. ssp. caffra
Pentanisia prunelloide	+	r + r				
Greyia sutherlandii	r	a				Greyia sutherlandii Hook. & Harv.
Haeman humili s. hirsu	+	r				Haemanthus humilis Jacq. ssp. hirsutus (Baker) Snijman
Eulalia villosa	r + r	a				Eulalia villosa (Thunb.) Nees
Sporobolus fimbriatus	+	+ + a				Sporobolus fimbriatus (Trin.) Nees
Scilla natalensis	r	r + + +		r		Scilla natalensis Planch.
Cheilanthes eckloniana			r			Cheilanthes eckloniana (Kunze) Mett.
Indigofera frutescens			r			Indigofera frutescens L.f.
Polygala virgata			r			
Galium capens s. garip		+	r r			Galium capense Thunb. ssp. garipense (Sond.) Puff
Aloe pratensis			r +			Aloe pratensis Baker
Heterorhachis aculeata			+			Heterorhachis aculeata (Burm.f.) Roessler
Helichrysum herbaceum		r	r +			Helichrysum herbaceum (Andrews) Sweet
Agrimonia procera	+ r	+	+ r			Agrimonia procera Wallr.
Berkheya setifera				r		Berkheya setifera DC.
Anemone fanninii		r		r		Anemone fanninii Harv. ex Mast.
Artemisia afra			a +	a a a		Artemisia afra Jacq. ex Willd.
Senecio speciosus	r + r r		r r	r r		Senecio speciosus Willd.
Vernonia hirsuta	r + +		r r	r r		Vernonia hirsuta (DC.) Sch.Bip. ex Walp.
Lotononis eriantha	a + a	+ r a +		a		Lotononis eriantha Benth.
Pteridium aquilinum	+ r	+ + a + +	+ a	a +		Pteridium aquilinum (L.) Kuhn
Acalypha wilmsii	a a + + r r	r + + + +	r +	+		Acalypha wilmsii Pax ex Prain & Hutch.
Acalypha angustata	a a r + a + + + +	+ r + + + + r	+	r + +		Acalypha angustata Sond.
Cyperus rupestris					+	
Geranium omithopodon					a	Geranium omithopodon Eckl. & Zeyh.
Cyperus dives					a	Cyperus dives Delile
Sporobolus africanus					+	Sporobolus africanus (Poir.) Robyns & Tournay
Gunnera perpensa				a a a	a b	Gunnera perpensa L.
Themeda triandra	b b b a b	a a a a + a	b b b	b	a +	Themeda triandra Forssk.

Although the role of vegetation in landsliding, through its influence on the hydrological cycle is recognised by most texts (e.g. Crozier, 1986; Selby, 1993) the detailed studies on the exact hydrological working are somewhat limited (e.g. Rebscher *et al.*, 1993). Studies usually focus on the commercial influence of vegetation on the hydrological cycle through vegetation clearing (Kuruppuarachi and Wyrowoll, 1992; Heiken, 1997) and veld burning (Cannon *et al.*, 1998), and are sometimes modelled for commercial purposes in a GIS (Miller and Sias, 1998). Vegetation also contributes to slope stability through roots (Neuland, 1976; Ziemer, 1981) that minimise sediment movement and erosion as shown in the studies by Gallart *et al.* (1993) and Sánchez and Puigdefabregas (1994). The rooting depth of most grasses in the study area S does not exceed 30cm and it is interesting to note that the failure plane for all the landslides in the area occurs beneath the rooting zones of the grasses. Added cohesion as a result of vegetation roots identified at depths up to 30cm (section 3.4.5.1).

3.4.2 Landslide relative age dating using vegetation recovery rates

For each of the landslides (section 3.2) the amount of vegetation recovery was estimated to give an indication of the relative-age of landslides scars (Appendix 2). Most grasses in area S are biennial species, which are able to germinate and be fully-grown within two years (Bijker *et al.*, 2001). The usefulness of vegetation recovery in the determination of the age of landslides lies in the fact that landslides remove all vegetation and leave a clean shear plane. The rate of landslide scar recovery is dependent on the slope gradient and disturbance, the local biotic factors such as dispersal and predation whilst competition of the vegetation play a less important role in scar rehabilitation Myster *et al* (1997). Figure 3.14 summarises the vegetation recovery in four arbitrarily chosen classes. Although the area is subject to occasional managed burning, the tussocks of most grasses stay intact and are accounted for in the estimation of recovery. Most of the landslide scars had more than a 60% vegetation recovery (Figure 3.14) and may be relatively old, probably 10 years or older. There is only one landslide with a recovery of less than 10%, which is assumed to be the most recent landslide in the study area.

Landslides in study area S, contain patches of vegetation surrounded by a matrix of soil or bare substrate and often undergo recurrent localised disturbance by resliding which adds new soil and organic material to the scar and removes vegetation. Vegetation regeneration of landslide scars takes place from the toe of the landslide,

where deposits of organic soil, broken plant parts and the most buried seeds are found (Guariguata, 1990). The upper sections of the landslides will take longer to recover, as seeds from adjacent areas must land and germinate.

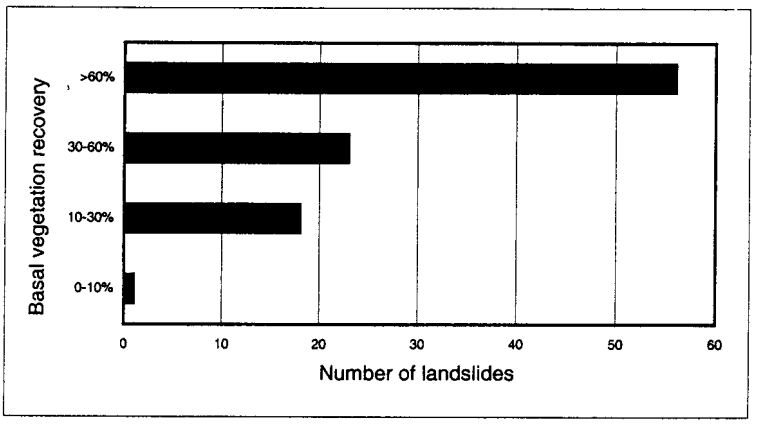

Figure 3.14: Basal vegetation recovery of landslide scars noted in study area S.

The dynamics of vegetation recovery following natural disturbances offers much scope for further research. Topics that have been researched include the effect of fire on old landslide scars (Walker and Boneta, 1995) and vegetation recovery rate following landslides and other geomorphic disturbances (Guariguata, 1990; Myster *et al.*, 1997; Myster and Walker, 1997; Robertson and Augspurger, 1999). The reason for scarcity of studies on the vegetation recovery associated with landslides is because landslides are usually studied in the context of posing a financial and social hazard to human beings (Chapter 1).

Apart form vegetation recovery rate, lichens have been used in numerous mass movement studies as a method for the relative age dating (e.g. Jonasson *et al.*, 1991; Bull *et al.*, 1994; McCarroll, 1994; Winchester and Harrison, 1994; Nicholas and Butler, 1996). Ages of surfaces are determined from the lichen growth rate, which is accepted to be constant under changing environmental conditions. However, McCarthy (1999) critically re-examined the biological basis for some key assumptions that were used to interpret lichen size-age data. It was found that most lichenometric ages are not verifiably accurate and that methodologies do not incorporate widely accepted biological principles. Lichen dating of landslides was not possible since most of the slides take place in soil and are seldom associated with rocks where lichen growth can take place as commonly cited in the Injisuthi Valley.

3.5 Summary

Morphometric analyses indicate that landslides in the study area are predominantly shallow translational, with landslides in the steep slopes being slightly larger than landslides located on riverbank slopes. Landslides tend to occur directly below the break of slopes and above the steeper sloping sections that do not contain enough soil to cause landslides. A rounded average of 100m^2 of soil is displaced by each landslide event, either to lower slopes or into streams.

Soil depth of the study area ranges between 0.1cm and 370cm with a computed average of 222cm and 95% of the area contains soil that are 222 ± 91cm deep. Soil type identification and textural analysis indicate that soil is vertically more heterogeneous than horizontally between different geological stratifications. The soil in the study area forms a catena that varies between Westleigh, Avalon and Longlands forms with the prominent characteristic being the orthic A horizon and a lower clay rich soft plintic B horizon. Textural differences between these horizons as well as average landslide scar depths show that the shear planes for landslides are between these two soil horizons, and not between the soil and the underlying geology as proposed previously.

Soil clay fractions were used to estimate the angle of internal friction from literature and an average of ϕ=31° will be used in the model as a constant (Table 3.1). Average bulk density was measured as 1.00±0.30g/cm^3 (converted to 1.0 x 10^{-4}KN/cm^3) and cohesion an average of 38kPa = 3.8 x 10^{-7} kN/cm^2 and the increased cohesion as a result of vegetation roots was included as a constant of 2.0 x 10^{-6} kN/cm^2 (Mulder, 1991).

Moisture content boundaries in the model were set to a minimum of 4%, a maximum of 43% and a soil moisture at field capacity of 10%. Soil infiltration capacity was correlated to slope angle and to soil texture (Briggs, 1977) and two main zones, the first on slopes ranging between 15° and 80° as 156cm/day and on slopes ranging between 0° and 15° as 288cm/day are included in the model. Further the vegetation assessed and the dynamics of vegetation recovery was used to give an indication of landslide age.

Local environmental properties, the measurements of which are described in this chapter, affect the timing, size and behaviour of shallow landslides in the Injisuthi Valley. Properties that were measured are inserted in the model as either constants or maps. Accuracy of the field measurements is of importance for the spatial accuracy of eventual model predictions, which can be assessed by comparing the model predictions to the GPS locations of the actual landslide observations, described in later chapters.